THE
PHYSICAL REVIEW
A journal of experimental and theoretical physics established by E. L. Nichols in 1893

SECOND SERIES, VOL. 67, NOS. 9 AND 10 MAY 1 AND 15, 1945

The Relativistic Increase in Ionization of High Energy Electrons and Mesotrons

WAYNE E. HAZEN
University of California, Berkeley, California
(Received March 12, 1945)

The ionization by electrons and mesotrons has been determined from drop counts along diffuse tracks that were photographed in a Wilson cloud chamber. It is believed that uncertainties in condensation efficiency and curvature do not contribute significantly to the errors. The relativistic increase in ionization for electrons agrees with theory but the average ionization of all penetrating particles is less than that predicted for a purely mesotronic composition. The minimum ionization by a singly-charged particle is 38 ion pairs per cm in dry air at N.P.T. when energy transfers greater than 600 ev are excluded.

SIMPLE considerations lead us to expect a decrease in the ionization by high speed charged particles as the speed increases. This expectation arises from the fact that the energy transferred to an electron by a passing charge depends on how long the Coulomb force acts on the electron. The higher the velocity of the passing charge, the shorter is the time the force acts on the electron, and the smaller is the energy transfer to the electron. But when the relativity contraction of the Coulomb field is taken into account, we find that the ionization should pass through a minimum for a kinetic energy of about $3m_0c^2$ and then increase slowly with further increase in energy[1] (see Fig. 2).

Thus far, cloud-chamber studies of the ionization or energy loss by cosmic rays have provided the only satisfactory method for studying the relativistic increase in ionization. Corson and Brode,[2] and J. G. Wilson[3] found some evidence for the increase but their experimental uncertainties were of the same order as the observed effect. A preliminary report of an experiment by Sen Gupta[4] indicates an increase for electrons and essentially none for mesotrons. Previous experiments by the author[5] have, more or less indirectly, shown evidence for no rise in the ionization. In the present work the ionization was obtained from drop counts along diffuse tracks photographed with a Wilson cloud chamber in a magnetic field.

EXPERIMENTAL METHOD

The photographs were obtained with a 7-cm by 30-cm cylindrical cloud chamber, which was placed in the gap of a large electro-magnet.[6] Since less than half the magnet coils could be used, the magnetic field was limited to 4500 gauss. Coincidence counters above and below the chamber initiated the operation of the ap-

[1] See B. Rossi and K. Greisen, Rev. Mod. Phys. **13**, 240 (1941).
[2] D. R. Corson and R. B. Brode, Phys. Rev. **53**, 773 (1938).
[3] J. G. Wilson, Proc. Roy. Soc. **A172**, 517 (1939).
[4] R. L. Sen Gupta, Nature **146**, 65 (1940).
[5] W. E. Hazen, Phys. Rev. **65**, 259 (1944).
[6] R. B. Brode, Science **93**, 435 (1941).

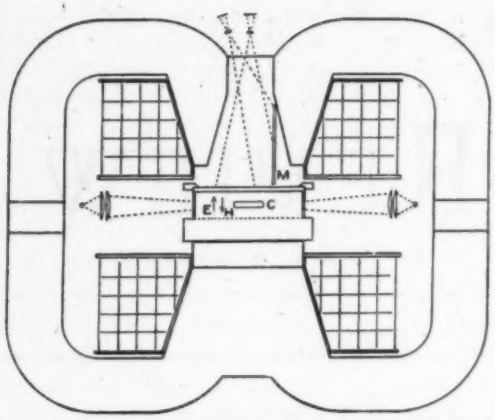

FIG. 1. A schematic drawing of the cloud chamber and magnet. The electric and magnetic field directions are indicated by E and H, the position of the counters by C, and the mirror by M. The angular fields covered by the cameras are shown by the dotted lines; in a vertical plane the angular fields were 40 percent greater and included all of the usable chamber height.

paratus. The time delay between passage of the cosmic ray and fixation of the ions by drop formation was 1/75 sec. in some of the photographs and 1/50 sec. in the remainder. Diffusion of the ions resulted in formation of ion columns with apparent diameters of 1.1 mm and 1.3 mm, respectively.

A uniform clearing field was obtained by aluminizing the front glass until its transmission was one-half and by maintaining a potential difference of about 50 volts between the front glass and the rear brass plate. The cosmic-ray track was thereby separated into parallel columns of plus and minus ions with a separation of 6 or 7 mm. No distortion of the track that was attributable to non-uniformity of the electric field could be detected with this electrode system. One picture was taken straight-on and a second by reflection in a front-surfaced mirror placed in the hollow pole piece of the magnet. Figure 1 is a schematic drawing illustrating the general arrangement of the apparatus. Illumination was provided by argon flash tubes as in previous work.[5]

Electrons with energies of 1–1.5 Mev were obtained from a P^{32} beta-ray source. The main modification in the experimental set-up consisted in the provision of a satisfactory substitute for the coincidence-counter method of timing the sequence of operations following the passage of a ray. The time tolerances are rather small for diffuse divided tracks suitable for ionization measurements. A rotating shutter was placed between the source and the aluminum-foil cloud-chamber window. Then a 1/50 sec. exposure of beta-rays could be obtained at the correct relative time by driving the shutter with a rotating shaft of the electro-mechanical device that timed the other cloud-chamber operations.

The ionization was determined from drop counts along the positive ion column in the reflected photograph. Inasmuch as the drops appeared nearly equally dense along the positive and negative columns of ions, there was considerable assurance that the condensation efficiency on positive ions was essentially 100 percent.[7] The drop counts were made from the negatives with a moving-stage microscope. Clusters containing more than 19–20 drops (gross number 30 drops minus 10–11 drops that normally occur in a cluster length of track) were omitted for the sake of accuracy in the drop counts and also because the rise in ionization is expected to be greater for small energy transfers. It was found possible to obtain satisfactory drop-image resolution with columns only slightly more than one-mm diameter in the chamber, or 0.12 mm on the film, and thus the accuracy of the curvature measurements was kept high. Indeed it requires very special care to obtain a counter-controlled track whose actual diameter is much less than one mm, as desired in cases where the curvature alone is to be measured.

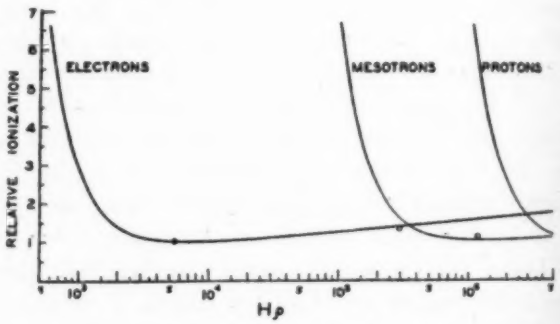

FIG. 2. Theoretical curves for the ionization by cosmic-ray particles including energy transfers less than 600 ev. The mesotron curve is for a mass of 180 m_e. The measured ionizations of the three monoenergetic groups (*a*), (*b*), and (*c*) are indicated by the small circles.

[7] C. E. Nielsen, Ph.D. Thesis, University of California, Berkeley (1941).

The curvatures were measured by direct comparison of the straight-on negative with a ruled transparent scale in the case of small radii and by a graph of readings taken with a micrometer-eyepiece travelling microscope in the case of large radii.[8] Magnification factors were determined from photographs of coordinate paper that was placed in the central plane of the counters. Since the region defined by the counters had a depth that was small compared with the camera distance, no correction was made for variations in camera to track distance arising from variations in longitudinal position of the tracks. In the reflected photograph, it was necessary to take into account the variation in magnification with lateral position, which arises from the tilted image plane.

RESULTS

The tracks were divided into four groups: (*a*) P^{32} beta-rays with $4500<H\rho<7000$ gauss-cm, (*b*) cosmic-ray electrons with $10^5<H\rho<8\times10^5$, (*c*) cosmic-ray mesotrons with $7\times10^5<H\rho<2\times10^6$, and (*d*) cosmic rays with $H\rho>7\times10^5$, few if any of which were electrons since all occurred singly. As illustrated in Fig. 2, group (*a*) is at the theoretical minimum of ionization for electrons, group (*b*) is in a region where theory predicts ionization 1.4 times the minimum, group (*c*) is at the minimum for mesotrons of mass 180 m_e, and group (*d*) includes essentially all of the penetrating component. The cosmic rays of group (*b*) were identified as electrons when $H\rho<2\times10^5$ on the basis of the fact that there is no evidence for mesotrons of mass as small as 120 m_e, which could have the same ionization as electrons at $H\rho=2\times10^5$. The other menbers of group (*b*) occurred as constituents of showers. They could not themselves have been mesotrons that produced knock-on electrons and subsequent showers because their energies were too low to account for the energies of the accompanying electrons. The distributions in ionizations of the tracks are shown in Fig. 3 and the mean values are listed in Table I. All the results for the ionization refer to events in which energy less than 600 ev was lost per collision by the ionizing particle, i.e., events in which the electron ejected by the ionizing particle produced fewer than 19 secondary ions. The results actually refer to ions of one sign, or ion pairs, and are reduced to number of ions per cm at N.P.T.

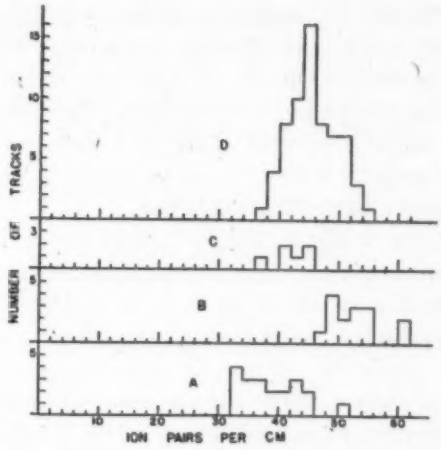

FIG. 3. Distribution curves for the measured values of the ionization by: (*a*) P^{32} beta-rays with $4500<H\rho<7000$, (*b*) cosmic-ray electrons with $10^5<H\rho<8\times10^5$, (*c*) cosmic-ray mesotrons with $7\times10^5<H\rho<2\times10^6$, and (*d*) cosmic rays with $H\rho>7\times10^5$ gauss-cm.

TABLE I. Ionization by electrons and mesotrons.

Particles group	Electrons *a*	Electrons *b*	Mesotrons *c*	Mesotrons *d*
$H\rho$ range (gauss-cm)	4500–7000	10^5–8×10^5	7×10^5–2×10^6	$>7\times10^5$
Ions per cm at N.P.T.	38.8	52.5	42.0	46.0
Corrected for resolution	42	56	45	49
Estimated probable error	2	3	3	2

The ionizations would be reduced by about 8 percent if referred to dry air.

Insofar as comparative results are concerned, it seems likely that the main uncertainty is in the statistical variation of the ionization events themselves. This conclusion is based on the fact that the probable error in a single observation as deduced from the scatter in the data is essentially equal to the probable statistical error in a single observation as deduced from the number of independent ionization events. For example, the ionization by the beta-rays of group (*a*) was 38.8 per cm but since the number of primary ions is 20 per cm,[9] the number of independent events is only one-half the counted number of

[8] P. M. S. Blackett and R. B. Brode, Proc. Roy. Soc. **A154**, 573 (1936).

[9] P. Kunze, Zeits. f. Physik **83**, 1 (1933).

ions. Since the counted number of ions per beta-ray track was 250, the probable statistical error is $0.67/(250/2)^{\frac{1}{2}}=6$ percent. From the observed scatter in the data the probable error is found to be 8 percent. Thus it is believed that in the present work the uncertainty as to condensation efficiency is negligible.

In order to obtain the best absolute values for the ionization, a correction should be made for overlapping of drop images. An overlap such that the image centers are separated by $\frac{3}{4}$ radius would probably result in the images being counted as one. With the narrow tracks used in these experiments, the resulting correction for overlapping of images is about 7 percent. The main uncertainty in determining absolute values is probably in the estimate of this overlap correction. In addition to the difficulty of determining the resolution criterion, there is the complication that many ions occur in clusters that are not due to fluctuations in independent events. If the results are to be reduced to ionization in dry air, there would be a decrease of 8 percent, which would approximately cancel with the resolution correction. It is believed that the final results have an uncertainty of perhaps 5 percent.

The results for electrons agree with theory well within the probable errors (Fig. 2) and the probable errors are several times smaller than the observed rise in ionization, thus confirming the relativistic rise in a convincing manner. Expressed numerically, the expected rise is 37 percent and the observed rise is 35 percent. The mesotrons of group (*c*) have an average ionization somewhat greater than the expected value but the number of tracks is small and the statistical uncertainty correspondingly large. The mesotrons of group (*d*) have a wide range of energies but the expected average ionization can be evaluated from the known spectrum.[5] Group (*d*) is expected to have a mean ionization 18 percent greater than the minimum whereas the experimental value is only twelve percent greater. This discrepancy in itself need not be regarded seriously since it is not much greater than the estimated probable error, but Sen Gupta[4] failed to observe any significant rise in ionization with energy for mesotrons at sea level and the author[5] failed to find the expected increase in ionization with filtration in 100 feet of rock. As previously suggested, it may be that there are more high energy protons in the cosmic radiation than is generally believed.

The present results for the average ionization by all the penetrating rays agree with those previously obtained[5] when the corrections for resolution and differences in upper limits of energy transfer are taken into account. In the previously reported experiments on the average ionization by the penetrating component, there was essentially no resolution correction since the tracks were very diffuse, but the upper limit of energy transfer was chosen at 800 ev. The Rutherford formula for probability $N(E)$ of energy transfer (E) in the region of 700 ev is[5]

$$N(E)dE=70dE/E^2 \text{ cm}^{-1} \text{ ev}^{-1}.$$

The ionization produced by events in the range of E from 600 to 800 ev would be

$$22\int_{600}^{800} N(E)dE,$$

which is about one ion per cm. Thus the result of the present experiment for the average ionization of the penetrating component including energy transfers up to 800 ev would be 50 ions per cm, in agreement with the earlier work.

It is believed that the best value to use for the minimum ionization by mesotrons in determinations of mass by the ionization-curvature method[2] is 42 ions per cm at N.P.T. for cases where clusters up to 20–30 ions (net) are included in the ion count. When corrected to dry air, this figure is reduced to 38 ions per cm.

This investigation was made possible through the use of Professor R. B. Brode's Carnegie magnet, which was financed by a grant from the Carnegie Institution of Washington.

Gamma-Rays Emitted During the Radioactive Transitions $Sb^{124} \rightarrow Te^{124}$ and $Na^{24} \rightarrow Mg^{24}$

P. GERALD KRUGER AND W. E. OGLE[1]
The Nuclear Radiation Laboratory, Physics Department, University of Illinois, Urbana, Illinois
(Received March 12, 1945)

Pair electrons observed in a cloud chamber provide the most accurate means of measuring gamma-ray energies, provided suitably rigid criteria of the selection of valid pairs are followed. The gamma-ray energies here reported were deduced from stereoscopic photographs of pair electrons formed in the gas of a cloud chamber. The magnetic field was known in absolute value to 1 percent or less and in relative value was constant to 0.2 percent or less. The radius of the electron tracks was measured by a special measuring engine. Careful collimation between the source and the cloud chamber was found necessary.

$Sb^{124} \rightarrow Te^{124}$

An examination of the gamma-rays emitted during the nuclear transition $Sb^{124} \rightarrow Te^{124}$ reveals a single monochromatic gamma-ray of energy 1.70 ± 0.02 Mev. This agrees with the beta-ray spectra observed by other experimenters. The pair production method of measuring gamma-ray energies is found to be accurate to ± 0.02 Mev provided care is taken in the selection of pairs.

$Na^{24} \rightarrow Mg^{24}$

Eleven thousand pictures yielded 56 pairs which satisfied the selection rules. Twelve of these pairs showed no observable scattering and indicate four gamma-ray lines at 2.56, 2.68, 2.76 and 2.89 Mev. Another pair indicates a weak line at 3.24 ± 0.1 Mev. These data are correlated with data on the beta-ray spectra and allow a term scheme for the nuclear transition $Na^{24} \rightarrow Mg^{24}$ to be proposed. The relative intensities of beta-ray and gamma-ray spectra are not incompatible, and the mass difference between the ground states of Na^{24} and Mg^{24} is in good agreement with the proposed term scheme.

THEORETICALLY the pair production method of measuring gamma-ray energies is ideal because of the high resolution which may be expected and the small number of observed pairs necessary to give a gamma-ray energy to within a few hundredths of a million electron volts. The method has been used in this laboratory[2] and has been tested by Groshev,[3] but it was thought worth while to do further work along these lines and to search for a radioactive source which emits a single monochromatic gamma-ray. From an examination of the literature it seemed that radioactive Sb and Na would be suitable sources to examine.

I. THE EXPERIMENTAL METHOD

The Wilson cloud chamber used in these experiments was eight inches in diameter and about one and one-half inches deep. It was constructed by W. E. Shoupp after the design of Crane.[4] The chamber was filled with air and a mixture of alcohol and water vapors, at atmospheric pressure. The ratio of alcohol to water was 3.5 to 1, and 27 cubic centimeters of liquid was used.

The field current was turned on eight seconds before expansion. In the runs on sodium it reached 74.8 amperes in about five seconds, and was held constant by an automatic regulator until about two seconds after the expansion. The regulator kept the current constant to ± 0.1 ampere. The ammeter used was calibrated by means of a standard resistance and a Wolff potentiometer and was found to read 75 when the current was 74.8 amperes. During the runs on antimony the current was kept at 49.9 amperes, which corresponds to a 50 amp. reading on the ammeter.

Stereoscopic pictures of the tracks were taken by a mirror system previously described.[5] An air-operated camera built by the University of Illinois physics department shop, and having an $f/2$ lens was used. The exposure time was between $\frac{1}{2}$ and $\frac{1}{10}$ of a second.

A G.E. high pressure mercury arc type H-6 was used as a source of illumination. The arc was run continuously, and a solenoid operated shutter was used to illuminate the chamber just before the expansion.

[1] Now engaged in military research.
[2] Kruger, Stallmann, and Shoupp, Phys. Rev. **56**, 297 (1939).
[3] Groshev, J. Phys. Acad. Sci. U.S.S.R. **5**, 135 (1941).
[4] Crane, Rev. Sci. Inst. **8**, 440 (1937).
[5] Kruger, Shoupp, and Stallmann, Phys. Rev. **52**, 678 (1937).

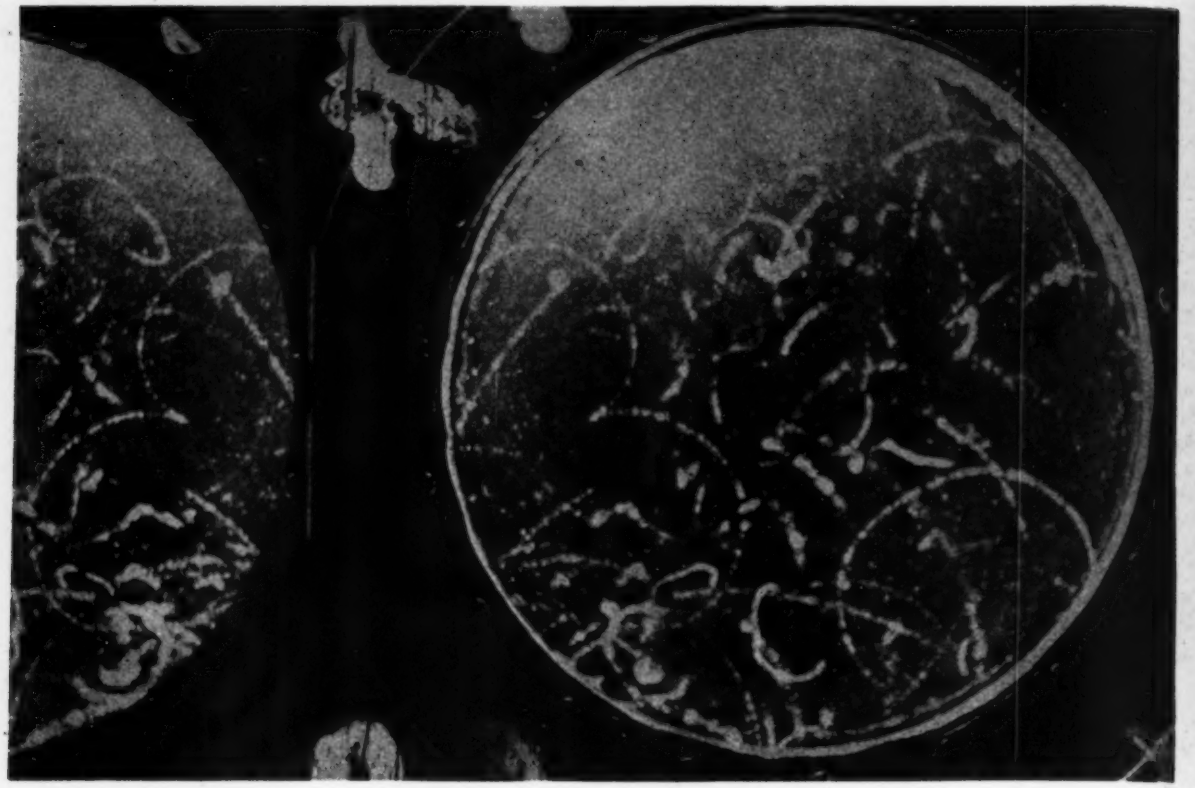

FIG. 1. Electron pair (No. 1 in Table I) produced by gamma-rays from radio-antimony. The magnetic field is 703 oersteds. The gamma-rays are collimated in the direction of the ruled lines which cross the picture and enter from the lower left side.

The Super XX film used was developed seven minutes in Kodak D-11, fixed 20 minutes in F-5, washed 30 minutes, wiped with viscose sponges and allowed to dry.

The gamma-rays were collimated perpendicular to the magnetic field and in the median plane of the cloud chamber by means of a slit 1″ wide, ½″ high, and 44″ long through a lead block. The region in which unscattered gamma-rays could form pairs in the chamber was outlined on the glass top of the chamber in ink so that it appeared in the pictures (Figs. 1 and 2). Pairs were readily located, since it was easy to see the positron track coming out of this region into a clear space relatively free of Compton electron tracks. There were a few Compton electrons, owing to scattered gammas from the wall of the chamber formed in the clear region to one side of the collimated beam, but this did not cause any confusion.

The pictures were examined first by means of a Spencer Delineascope and any possible pairs picked out. These pictures were marked. Then they were projected through the same optical system of camera and mirrors with which the pictures were taken. The pictures were brought into focus on a ground glass screen and a careful examination of each pair was made.

The criteria used to select a pair as valid data are as follows:

1. Both tracks must be in the same plane, and that plane must lie within 10° of a plane through the median plane of the cloud chamber and perpendicular to the magnetic field.
2. Both tracks must lie within a 20° solid cone of the forward direction.
3. The initial angle between the paths of the pair electrons must be less than 25° unless the electron has so much more energy than the positron that large angle scattering can be ruled out.
4. Both tracks shall start at the same point and be of the same age as determined by the diffuseness of the track.
5. There can be no obvious scattering in the track over the region in which the radius of curvature is measured.

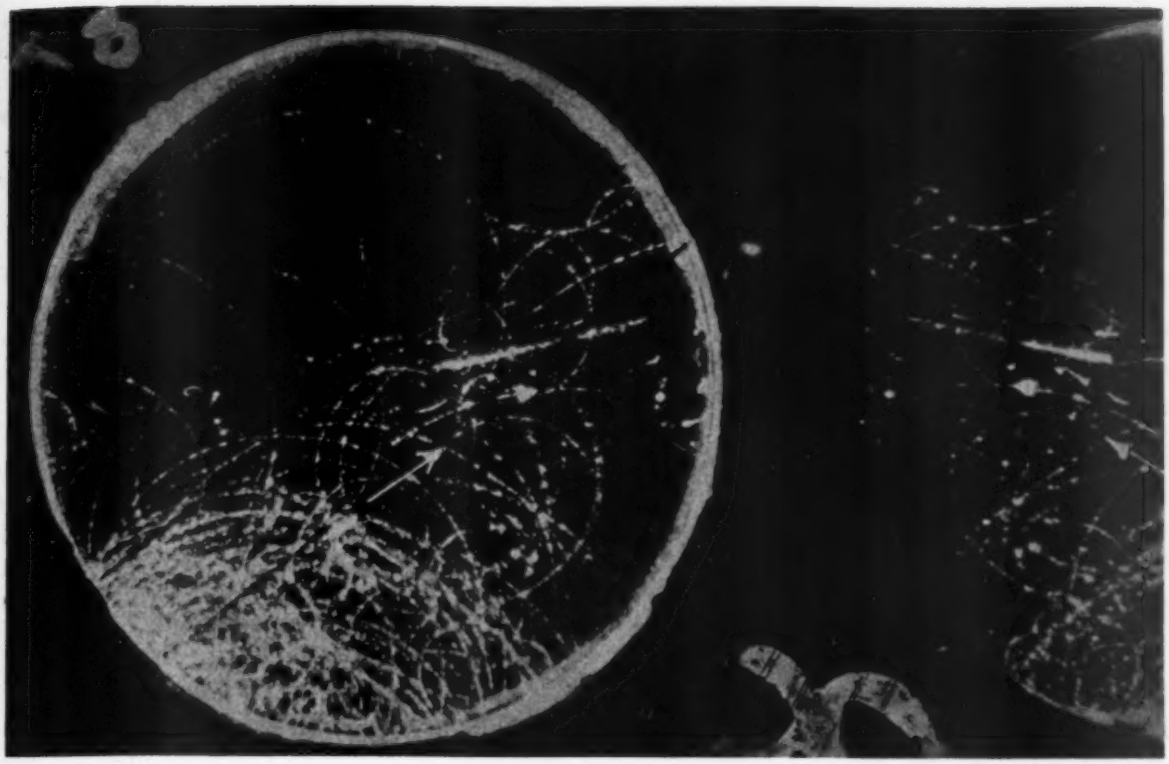

FIG. 2. Electron pair (No. 89 Class AA, Table III) produced by gamma-ray from radium-sodium. The magnetic field is 1055 oersteds. Other conditions are the same as those in Fig. 1. The effect of collimation is clearly evident.

A measuring engine which determined the chord and the sagitta of the arc of the track was used to find the radius of curvature of each track. The engine was calibrated by means of a comparator. The radius of curvature of an electron track is given by

$$r=(c^2/4+s^2)/2s,$$

where c is the length of the chord and s is the corresponding sagitta length.

Several (two or more) independent sets of measurements on each pair were taken and the probable error in measurement for each pair was calculated from these data. The pairs were then ranked inversely as their probable error, and weighed accordingly.

The energy of the gamma-ray is then given by

$$E=mc^2[(B_1^2+1)^{\frac{1}{2}}+(B_2^2+1)^{\frac{1}{2}}],$$

where

$$B=Hre/mc^2,$$

and the subscript 1 refers to the electron and 2 to the positron. Here Hr is the product of the radius of curvature of the track and the magnetic field strength, e is the charge on the electron, and mc^2 is the self-energy of the electron. In these calculations the following values were used:

$$mc^2=81.83\cdot10^{-8}\text{ ergs}=0.5108\text{ Mev.}$$
$$e=4.8025\cdot10^{-10}\text{ e.s.u.}$$

The magnetic field caused by the cloud chamber coils was measured by a method involving the use of a flip coil, 6″ in diameter, connected in series with a standard mutual inductance and a ballistic galvanometer whose period was long compared to the time necessary to flip the coil. The breaking of a known current in the primary of the mutual inductance produced a deflection of the galvanometer that could be compared to the deflection produced by flipping the coil in the magnetic field. From these data the field intensity was calculated. The area of the flip coil was known with an error of less than 0.1 percent. The standard mutual inductance was calibrated by the National Bureau of

TABLE I. Pairs produced by gamma-rays from the nuclear transition $Sb^{124} \rightarrow Te^{124}$.

Pair number	Pair class	Hr^+	Hr^-	E^+ Mev	E^- Mev	E Mev
1	*C*	1974	2527	0.271	0.403	1.70±0.03
2	*B*	1959	2570	0.267	0.414	1.70±0.02
3	*AA*	1355	3046	0.142	0.535	1.699±0.002
4	*A*	2383	2289	0.367	0.345	1.73±0.01
5	*D*	1915	2345	0.258	0.359	1.64±0.05

Standards. Magnetic field measurements were made at 74.8 amp. before the pictures were taken and were checked at 74.8 amp. and 49.9 amp. at the end of the experiment. These measurements gave field values of 1055±0.4 percent oersteds at 74.8 amp. and 703±0.4 percent oersteds at 49.9 amp. Thus, the absolute value of magnetic field should be accurate to 1 percent.

II. THE GAMMA-RAY SPECTRUM OF $Sb^{124} \rightarrow Te^{124}$

The gamma-rays from $Sb^{124} \rightarrow Te^{124}$ have been examined by Mitchell, Langer, and McDaniel,[6] and by Klaiber and Scharff-Goldhaber[7] who reported 1.82 Mev and 1.75 Mev respectively for the gamma-ray energy. The beta-ray spectrum has been examined by Mitchell, Langer, and McDaniel,[6] and by Hales and Jordan,[8] the latter reporting beta-rays of 0.74 Mev and 2.45 Mev, so that a single gamma-ray of energy 1.71 might be expected.[9] The establishment of a standard monochromatic gamma-ray source would be valuable in many nuclear physics experiments.

The radioactive Sb was prepared in this laboratory by bombarding chemically pure Sb powder with 10-Mev deuterons. The estimated bombardment was 600±200 μamp. hours. In such a bombardment the following nuclear reactions may take place:

$$Sb^{123}(d, p)Sb^{124};\ Sb^{123}(d, n)Te^{124};\ Sb^{121}(d, p)Sb^{122};\ Sb^{121}(d, n)Te^{122};\ Sb^{121}(d, 2n)Te^{121}.$$

Thus, after bombardment, it was necessary to separate chemically the radioactive Te from the radioactive Sb. After separation the Sb source was aged for 2 weeks to reduce the Sb^{122} (2.8 day half life) to less than 1/50 of its original activity. A measurement of the activity of the Sb source after ageing showed that about 1 mC of radio antimony was obtained.

Twelve thousand pictures taken with the Sb source in the Pb collimator and 50-cm distance from the cloud chamber, yielded the five pairs listed in Table I. The magnetic field was 703 oersteds.

The error given is the probable error, calculated from several measurements on the same pair made along different parts of the positron and electron tracks. That is, the radius of curvature was measured close to the vertex, further along close to the center, and at the end of the track. Thus, the probable error, as given, is a measure of the error introduced by small angle scattering. These probable errors are in agreement with that which would be expected from the theory of small angle scattering. The weighted (see weights in the sodium data) average value of E_γ from the data in Table I is 1.70±0.01 Mev. Since the magnetic field has a probable error of one percent, the absolute value of E_γ is 1.70±0.02 Mev.

Of the pairs reported in Table I, numbers 1, 2, and 3 satisfy all of the criteria set forth above. Pair No. 4 satisfies all criteria except criterium No. 2, i.e., pair No. 4 was formed in the backward direction. Pair No. 5 satisfies all criteria except criterium No. 5. Because of the relatively large probable error it is clear that serious small angle scattering has occurred. The pair classification in Column 2 of Table I is made on the basis of the probable error for each track.

From these data it is clear that with careful selection of tracks following the criteria stated above, the spread of pair energies from a monochromatic gamma-ray is small, in this case 0.01 Mev so that it is possible to resolve gamma-ray lines as close as 0.05 Mev apart.

In conclusion, from the data of Hales and Jordan[8] and from these data, it appears that Sb^{124} decays with two beta-rays, one to the ground state of Te^{124} and one to an excited state of Te^{124} which is 1.70 Mev above the ground state. The

[6] Mitchell, Langer, and McDaniel, Phys. Rev. **57**, 1107 (1940).
[7] Klaiber and Scharff-Goldhaber, Phys. Rev. **61**, 733 (1942).
[8] Hales and Jordan, Phys. Rev. **62**, 553 (1942).
[9] Because of the 0.069 Mev gamma-ray reported by Mitchell, *et al.*, there is the possibility of a gamma-ray at 1.78 Mev, which from our data, if it exists, must be less than ½ as intense as the 1.71 Mev line.

observed gamma-ray of 1.70 Mev results from a transition from the excited state of Te^{124} to the ground state of Te^{124}. The gamma-ray apparently is monochromatic.

The energy of the Sb gamma-ray here reported is also in agreement with that reported by Scharff-Goldhaber and Klaiber.[10] They deduced the gamma-ray energy from energy measurement on recoil protons, produced by photo-neutrons which were ejected from beryllium by gamma-rays from radio-antimony. The value they obtained was 1.75 ± 0.04 Mev.[11]

Fig. 1 shows a picture of a pair produced by Sb gamma-rays.

III. THE GAMMA-RAY SPECTRUM OF $Na^{24} \rightarrow Mg^{24}$

The gamma-rays of Na^{24} have been studied by many investigators[12–18] who have reported various gamma-ray energies between 0.8 Mev and 3.0 Mev. Only recently have the reported γ-ray energies come into near agreement. For this reason it was considered advisable to make another study, employing the pair production method, to determine the gamma-ray energy more accurately and to see if the gamma-ray lines were single or complex.

The Na^{24} used in these experiments was produced by bombarding c.p. NaF with 10-Mev deuterons in this laboratory. Each bombardment yielded about 200 mC of Na^{24}. Radioactive F^{20} was produced at the same time by the d, p reaction. The source was aged about an hour before pictures were taken, and it was used until it decayed to about 30 mC. The half-life of radioactive fluorine is about 13 seconds, so no contamination should be introduced by the fluorine.

With the sodium source placed in the lead collimator at an average distance of 1 meter from the cloud chamber, 11,000 pictures were taken. These yielded about 200 pairs, of which 56 satisfied the selection rules and were accepted

TABLE II. Experimental data on positron-electron pairs (Mg^{24} gamma-rays).

E^+ is the kinetic energy of the positron in Mev.
E^- is the kinetic energy of the electron in Mev.
E_γ is the energy of the gamma-ray from E^+ and E^-.

Pair number	E^+	E^-	$E^+/(E^+ + E^-)$	E_γ
15	0.749	0.994	0.45	2.76
17*T*	0.425	0.978		2.68
		0.259		
18	0.816	1.017	0.445	2.85
19	0.523	1.158	0.31	2.70
21	0.979	0.535	0.64	2.54
22	1.758	0.101	0.95	2.88
23	0.941	0.691	0.58	2.65
24	0.520	1.161	0.31	2.70
25	0.488	1.007	0.32	2.52
26	1.348	0.519	0.72	2.89
29	0.806	0.671	0.54	2.50
30	0.526	0.854	0.382	2.40
31	1.446	0.205	0.88	2.67
33	0.607	1.145	0.35	2.77
34	1.056	0.512	0.68	2.58
35	1.256	0.507	0.71	2.78
38	1.206	0.453	0.73	2.68
42	0.633	0.930	0.40	2.58
43	1.170	1.048	0.53	3.24
44*T*	0.674	0.900		2.66
		0.067		
45	0.871	0.660	0.57	2.55
49	0.767	0.808	0.49	2.60
51	0.849	0.804	0.51	2.68
53	0.391	1.318	0.23	2.73
54	1.285	0.459	0.73	2.77
56	0.803	0.913	0.47	2.74
57	0.152	1.714	0.08	2.89
58	0.627	0.899	0.41	2.55
61	0.412	1.120	0.27	2.55
62	0.498	1.013	0.33	2.53
63	0.436	1.129	0.28	2.59
66	1.432	0.150	0.904	2.60
67	0.511	0.998	0.34	2.53
69	0.290	1.238	0.19	2.55
70	1.439	0.260	0.85	2.72
71	0.703	0.985	0.42	2.71
73	0.787	0.972	0.45	2.78
74	1.450	0.094	0.94	2.57
77	0.554	1.164	0.32	2.74
78	1.335	0.325	0.81	2.68
79	0.902	1.040	0.47	2.96
80	0.933	0.712	0.57	2.67
83	1.357	0.400	0.79	2.78
84	1.104	0.340	0.76	2.47
85	0.735	0.829	0.47	2.59
86	0.857	0.941	0.48	2.79
87	0.394	1.328	0.23	2.74
89	1.435	0.476	0.75	2.93
90	1.424	0.282	0.83	2.73
91	1.472	0.351	0.81	2.85
92	0.985	0.520	0.65	2.53
94	0.502	1.241	0.29	2.77
97	0.605	0.954	0.39	2.58
99	0.678	0.930	0.42	2.63
100	0.269	1.586	0.145	2.88

[10] Scharff-Goldhaber and Klaiber, Phys. Rev. **61**, 733A (1942).
[11] The probable error given by Goldhaber in private communications.
[12] Richardson and Kurie, Phys. Rev. **50**, 1004 (1936). Richardson, Phys. Rev. **53**, 124 (1938).
[13] J. Itoh, Proc. Phys. Math. Soc. Japan **23**, 605 (1941).
[14] Curran, Dee, and Strothers, Proc. Roy. Soc. **A174**, 546 (1940).
[15] Mandeville, Phys. Rev. **62**, 309 (1942); Phys. Rev. **62**, 555 (1942); Phys. Rev. **63**, 91 (1943); Phys. Rev. **63**, 387L (1943).
[16] Elliot, Deutsch, and Roberts, Phys. Rev. **63**, 386L (1943).
[17] M. Goldhaber, Klaiber, and G. Scharff-Goldhaber, Phys. Rev. **65**, 61A (1944).
[18] A preliminary report on the data in this paper was given previously. W. E. Ogle and P. G. Kruger, Phys. Rev. **65**, 61A (1944).

TABLE III. Positron-electron pairs arranged according to energy and probable error (Mg^{24} gamma-rays).

Class AA—Very best pairs. No observable scattering.
Class A—Probable error 0.01 Mev.
Class B—Probable error 0.02 Mev.
Class C—Probable error 0.03 Mev.
Class D—Probable error 0.04 Mev or greater.
T indicates "Triplets."
Values given in million electron volts.
( ) Give pair number.

Class AA	(69) 2.55	(19) 2.70	(83) 2.78	(89) 2.93
	(21) 2.54	(31) 2.67	(77) 2.74	(57) 2.89
	(67) 2.53	(17) 2.68*T*	(73) 2.78	
		(44) 2.66*T*		
Class A	(42) 2.58	(24) 2.70	(33) 2.77	
	(45) 2.55	(38) 2.68		
	(49) 2.60			
Class B	(62) 2.53	(51) 2.68	(15) 2.76	(18) 2.85
	(66) 2.60	(78) 2.68		(26) 2.89
	(58) 2.55	(70) 2.72		
	(97) 2.58			
	(30) 2.40			
	(84) 2.47	(99) 2.63		
Class C	(61) 2.55	(71) 2.71	(35) 2.78	(22) 2.88
	(85) 2.59		(53) 2.73	
	(74) 2.57		(86) 2.79	
	(63) 2.59		(54) 2.77	
	(92) 2.53		(87) 2.74	
			(90) 2.73	
Class D	(29) 2.50	(23) 2.65	(56) 2.74	(79) 2.96 (43) 3.24±0.1
	(34) 2.58	(80) 2.67	(94) 2.77	(91) 2.85
	(25) 2.52			(100) 2.88

as valid data. Figure 2 shows a typical pair produced by Na gamma-rays. Data on these pairs are shown in Tables II and III. Table II gives the energy of the electron (E^-) in million electron volts, the energy of the positron (E^+) of the same pair, the ratio $E^+/(E^++E^-)$, and the gamma-ray energy calculated from those data. The *T* indicates that numbers 17 and 44 are triplets; i.e., pairs produced in the field of an electron.

It is of interest to compare the experimental distribution of $E^+/(E^++E^-)$ with the theoretical distribution calculated by Heitler.[19] E^+ is the kinetic energy of the positron of a pair, and E^- is the kinetic energy of the electron of the same pair. The theoretical curve of number of pairs *vs.* $E^+/(E^+-E^-)$ is shown by the solid curve in Fig. 3 for a gamma-ray in the energy region of 2.7 Mev. The curve is normalized to the number of pairs observed. The experimental points are plotted on the same graph, and the probable error ($\sqrt{N}$) is shown by the length of the vertical line going through the experimental point. The observed distribution of $E^+/(E^++E^-)$ is not in disagreement with the theoretical distribution as given by Heitler.

The pair energies, as calculated from the observed data, spread over the region from 2.4 to 3.24 Mev. From the theory of pair production one would expect to obtain the true energy of the gamma-ray from the measurements on a single ideal pair; i.e., a pair that has suffered no scattering. The pair energies obtained during the measurements of the gamma-ray from the decay of Sb^{124} were all within 0.03 Mev of each other, with the exception of one pair (No. 5, Table I) that was very badly scattered.

Since the scattering of the electrons is a multiple process, with just as much chance of scattering to one side as to the other side, one should sometimes be able to find tracks that are scattered just as much to one side as to the other, so that the effective scattering is zero. Then if one measures the radius of curvature of that electron track in a magnetic field one should be able to calculate the energy very accurately. A

[19] Heitler, *The Quantum Theory of Radiation* (Oxford University Press, New York, 1936), p. 199.

track that would satisfy the above criteria then would be one that was long enough so that one could make several measurements of the radius of curvature along the length of the track, and such that those measurements would all show the same radius of curvature. From the data on Sb^{124} it appears that such tracks are possible. The 56 pairs due to the Na^{24} gamma-rays were very carefully inspected and 12 satisfied the above criteria. Those 12 are listed in the top (AA) section of Table III. They seem to fall into four groups of pairs. The four groups have average energies of 2.54, 2.68, 2.77, and 2.91 Mev. Thus, it seems that the gamma-ray spectrum of $Na^{24} \rightarrow Mg^{24}$ is complex and that there are four gamma-ray lines in the region from 2.4 to 3.0 Mev.

The rest of the pairs are arranged in Table III in columns corresponding to that energy group with which they are in closest agreement. They are also arranged in rows according to their probable error in measurement as indicated by the general appearance of the pair (length of track, evidence of scattering) and by the spread in energy measurements made on different parts of the tracks. The second or A section of Table III gives those pairs such that the probable error from several measurements is about ± 0.01 Mev, B section lists those such that the probable error is about ± 0.02 Mev, C section lists those with a probable error of ± 0.03 Mev, and D section lists those with a probable error of ± 0.04 Mev or greater. The pairs in sections B and D probably do not improve the value of the energy of the group, but their number is useful in estimating the intensity of the gamma-ray line. The energies of the pairs in each group were averaged weighing the AA pairs five times, the A pairs four times, the B pairs three times, and the C pairs twice as much as the D pairs.

It is possible that pairs numbers 30 and 84 indicate a lower energy gamma-ray line, but since they are not really first class pairs no particular importance is attached to them. Number 99 was right between two energy groups, so it was not assigned to either one of them. It is not a really first class pair so no importance is attached to the fact that it lies right between two of the energy groups indicated by the AA pairs. Possibly numbers 30, 84, and 99 are among the 5 or 6 percent of the pairs that one would expect to be formed by gamma-rays that are scattered by the glass wall of the cloud chamber in such a manner that they still get into the cloud chamber. Pair number 43 indicates the possibility of a very weak gamma-ray at about three and a quarter million electron volts.

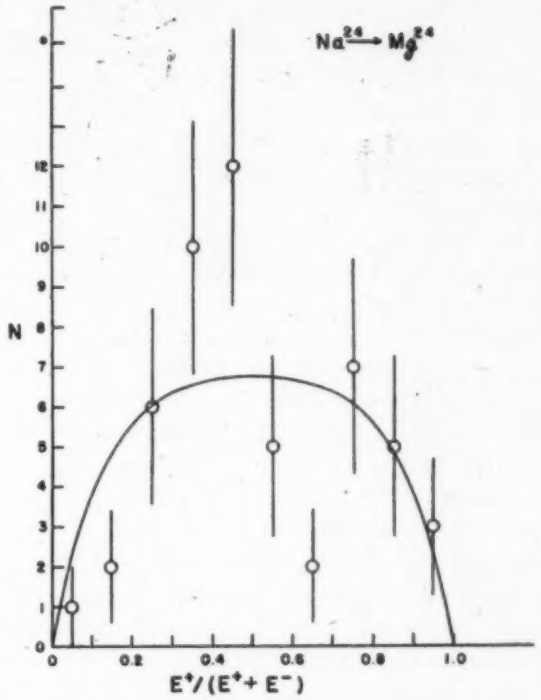

FIG. 3. The number of pairs having a given value of $E^+/(E^+ + E^-)$ is plotted against the value of $E^+/(E^+ + E^-)$. The solid curve represents the theoretically predicted distribution. These data represent the pairs produced by radio-sodium gamma-rays.

In order to estimate the intensities of the gamma-ray lines observed by the method of pair production one must take into account the variation of pair production probability with the energy of the incident gamma-ray. The number of pairs produced per unit time by a monochromatic gamma-ray of intensity I will be proportional to the product of the intensity and the pair production probability at that energy. So if one divides the number of pairs observed for each gamma-ray line by the pair production probability at that energy (taken from Heitler)[20] one obtains a number that is proportional to the intensity of that gamma-ray line. These data for Na^{24} are given in Table IV.

[20] Heitler, p. 201 (see reference 19).

Thus, these data indicate the existence of four gamma-ray lines due to the radioactive decay of Na^{24}, with the possibility of a weak fifth line. Their energies are 2.56 ± 0.02 Mev, 2.68 ± 0.02, 2.76 ± 0.02, 2.89 ± 0.03, and 3.24 ± 0.1 Mev; of relative intensities 26, 15, 16, 9.0, 0.9, respectively.

Other investigators[15,16] report, in addition to a gamma-ray of about 2.8 Mev, a line at 1.38 Mev. Because of the decrease of pair production probability with decreasing gamma-ray energy, the pair production method probably would not show such a gamma-ray line unless it were very intense as compared to higher energy lines. The 1.38 Mev line is reported to be about the same intensity as the line at 2.80 ± 0.1 Mev. The pair production probability at 1.38 Mev is about 1/16 that at 2.8 Mev. The present investigation would thus expect to find three pairs of that energy. None was observed, possibly because such pairs would have electron tracks with very small radii of curvature, and might easily be mistaken for scattering, since probably the whole pair would be in the gamma-ray beam.

The gamma-ray energies reported here are not incompatible with the results of other recent investigations. Elliott, Deutsch and Roberts[16] report two lines at 1.38 and 2.76 ± 0.01 Mev. The 2.76 Mev line is in agreement with the 2.76 Mev line of this paper. That measurement was made by means of observing the end point of a Compton electron distribution and also the photoelectron peak with a magnetic spectrograph. The half-width of the photoelectron peak was 3.5 percent. The photoelectron peak would probably show up the strong line at 2.76 Mev, and the weaker line at 2.89 Mev would possibly not be noticed. Mandeville[15] reports two lines at 1.38 and 2.94 ± 0.05 Mev. The 2.94 Mev value is the end point of a Compton electron distribution as measured with a magnetic spectrograph. That value is in essential agreement with the 2.89 Mev line of this paper. The close lines of about the same intensity would possibly not be resolved by the spectrograph.

Goldhaber, Klaiber, and Scharff-Goldhaber[17] have reported a line at 2.87 ± 0.05 Mev agreeing with the 2.89 Mev line of the present paper, and measured by observing the end point of the distribution of recoil protons in an ionization chamber. The recoil protons are produced by neutrons from the photo-disintegration of beryllium and deuterium.

The beta-ray spectrum of Na^{24} has been investigated by several workers. Feather and Dunworth[21] investigated the spectrum by absorption methods, and reported one beta-ray at 1.4 ± 0.05 Mev. From coincidence measurements they think there is more than one gamma-ray per beta-ray. Amaki and Sugimoto[22] using a Wilson cloud chamber, report two beta-rays at 1.24 and 0.29 Mev.[23] The relative intensities were given as 4.9 to 1 respectively. Kurie, Richardson, and Paxton[24] reported a beta-ray between 1.43 and 1.18 Mev,[23] and also suggested the possibility of a lower energy beta-ray. Lawson,[25] using a magnetic spectrograph, found evidence of a single beta-ray at 1.4 Mev.[23] Kikuchi, *et al.*[26] measured the beta-ray spectrum with a magnetic spectrograph and found an upper limit of the spectrum at 1.37 Mev.[24] However, the Fermi plot of their data, which should be a straight line if there is only one beta-ray, is kinked, indicating beta-rays at 1.84, 1.63, and 1.07 Mev (including the rest mass), of relative intensities 515:160:40, respectively. Konopinski and Uhlenbeck[27] find that the Na^{24} beta-ray spectrum may be complex. The coincidence measurements of Langer, Mitchell, and McDaniel,[28] and of Watase[29] indicate that at least two quanta are successively emitted after each beta-disintegration.

TABLE IV.

Gamma-ray energy (Mev)	Relative pair production probability	Number of pairs observed	Relative gamma-ray intensity
2.56	0.70	18	26
2.68	0.78	12	15
2.76	0.82	13	16
2.89	0.88	8	9.0
3.24	1.07	1	0.9

[21] Feather and Dunworth, Proc. Camb. Phil. Soc. **34**, 442 (1938).
[22] Amaki and Sugimoto, Sci. Pap. Inst. Phys. and Chem. Res. (Tokyo) **34**, 1650 (1938).
[23] Beta-ray value does not include rest mass.
[24] Kurie, Richardson, and Paxton, Phys. Rev. **49**, 375 (1936).
[25] J. L. Lawson, Phys. Rev. **56**, 131 (1939).
[26] Kikuchi *et al.*, Physico Math. Soc. Japan **21**, 381 (1939).
[27] Konopinski and Uhlenbeck, Phys. Rev. **60**, 308 (1941).
[28] Langer, Mitchell, and McDaniel, Phys. Rev. **56**, 962 (1941).
[29] Watase, Physico Math. Soc. Japan, **23**, 618 (1941).

The results of the last three papers above and of the present work suggest the term scheme for the decay of Na^{24} to Mg^{24} shown in Fig. 4. It is proposed that Na^{24} decays with the emission of three beta-rays of energies (including mc^2) of 1.84, 1.63 and 1.07 Mev to three excited levels of Mg^{24} at 3.94, 4.14, and about 4.70 Mev, respectively. These levels in turn decay by gamma-emission to two levels at 1.38 and 1.26 Mev. That is, the level at 4.70 Mev, which has a very weak population according to Kikuchi, decays with the emission of a weak gamma-ray of about 3.24 ± 0.1 Mev to the level at 1.38 Mev. The Mg^{24} level at 4.14 Mev above ground decays with the emission of two gamma-rays of energies 2.89 and 2.76 Mev to levels at 1.26 and 1.38 Mev respectively. Likewise, the level at 3.94 Mev decays with the emission of two gamma-rays of energy 2.56 and 2.68 Mev to the levels at 1.38 and 1.26 Mev. The levels at 1.38 and 1.26 Mev then decay by gamma-emission to the ground state of Mg^{24}. The gamma-ray of energy 1.26 Mev has not been reported by other investigators, and would not be observed in the course of the present investigation. However, from the above data that line would be about as intense as the line at 1.38 Mev, and only 0.12 Mev away from it, and hence might not have been resolved.

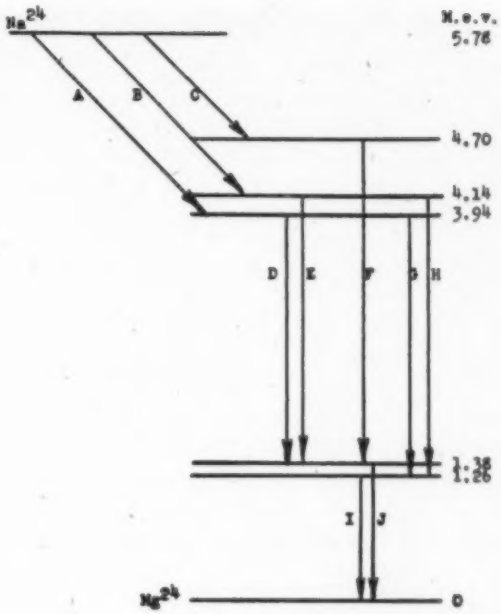

Line	Energy Mev	Relative intensity
	Beta-Ray Spectra	
A	1.84	515
B	1.63	160
C	1.07	40
	Gamm-Ray Spectra	
D	2.56	26
E	2.76	15
F	3.24	0.9
G	2.68	16
H	2.89	9
I	(1.26)	(25)
J	1.38	42

FIG. 4. Proposed term scheme for the nuclear transition $Na^{24} \rightarrow Mg^{24}$. Lines *I* and *J* have been observed as a single line by other investigators and no data on these lines are reported in this paper.

In order for the term scheme of Fig. 4 to be reasonable the intensities of the various gamma-rays should correlate with the populations of the levels expected from beta- and gamma-ray measurements. Other investigators report that the gamma-ray of energy 1.38 Mev is of about the same intensity as the line they observe at about 2.8 Mev. If that line is actually complex as indicated by the present work, and is made up of gamma-rays as indicated by Fig. 4, the sum of the individual intensities of the high energy gamma-rays would add up to the sum of the low energy gamma-ray intensities, as reported. The populations of the Mg^{24} levels at 3.94, 4.14, and 4.71 Mev from the beta-ray spectrum observed by Kikuchi are about 13:4:1, respectively. The populations of the same levels estimated using the gamma-ray intensities given in Table IV are in the ratio of $42\pm11:24\pm8:0.9\pm1$. By assuming the most favorable limits of error the ratios can be written 53:16:0.2; which is 13.4:0.5 and which is not incompatible with Kikuchi's results. The proposed term schene would place the ground state of Na^{24} 5.78 Mev above the ground state of Mg^{24}.

The theoretical work of Barkas[30] predicts atomic masses of Na^{24} and Mg^{24} of 23.9974 and 23.9920 atomic mass units, respectively. The difference between these two values is 0.0054 mass unit, or 5.03 Mev. Thus the energy difference between the nuclear ground levels should be 5.03 Mev. The present work gives 5.78 Mev but this value includes mc^2 for the beta-ray. Therefore, the value to be compared with 5.03 Mev is 5.78 Mev minus mc^2, which equals 5.27 Mev. This is in good agreement with the value obtained from the mass difference.

[30] Barkas, Phys. Rev. **55**, 691 (1939).

Pair Electrons Formed in the Field of an Electron

W. E. OGLE* AND P. GERALD KRUGER
The Nuclear Radiations Laboratory, Physics Department, University of Illinois, Urbana, Illinois
(Received March 12, 1945)

The observation of pair electrons which were formed in the field of an electron is reported. These triplets were photographed in a cloud chamber which was irradiated with gamma-rays from radioactive sodium. Measurements on the tracks of the triplets show that energy and momentum are conserved in the process.

THE theory of pair production in the field of an electron was first considered by Perrin,[1] who calculated that the threshold for the process is 4 mc^2. Since in this case one observes the recoil electron as well as the positive-negative electrons of the pair, the three observed particles are often referred to as a triplet.

DaSilva[2] believes to have observed a triplet which was produced in a lead foil. This case is not completely satisfactory since the vertex of the triplet was in the lead foil and, therefore, not clearly visible. Shinohara and Hatoyama[3] report the observation of a triplet formed in the air of a cloud chamber but, in the photograph pub-

* Now engaged in military research.
[1] F. Perrin, Comptes rendus **197**, 1100 (1933).
[2] A. M. DaSilva, Comptes rendus **206**, 1365 (1938).
[3] K. Shinohara and M. Hatoyama, Phys. Rev. **59**, 461 (1941).

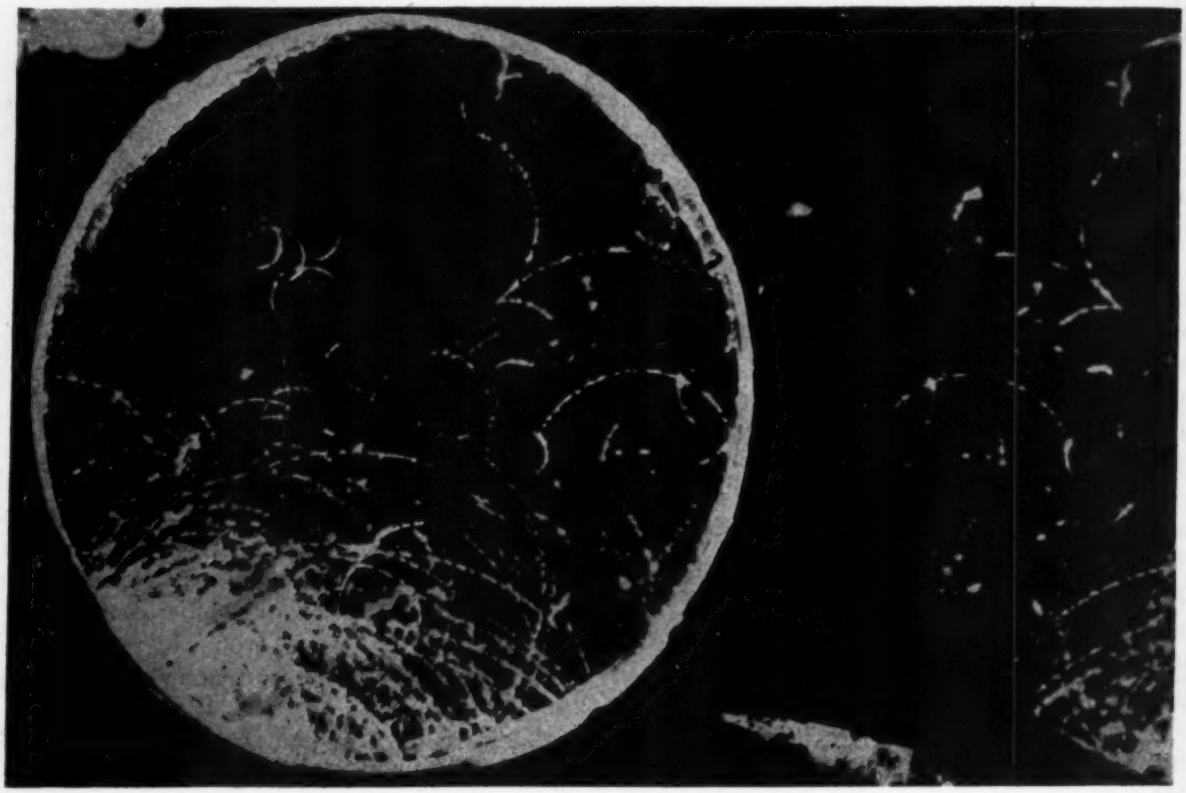

FIG. 1. Triplet No. 1. The direct image and one-half of the stereoscopic view are shown. The triplet is visible in the upper right quadrant of the direct view and in the corresponding section of the stereoscopic view. From both views it is clear that all three tracks of the triplet have a common origin. The gamma-rays enter the cloud chamber from the lower left-hand quadrant.

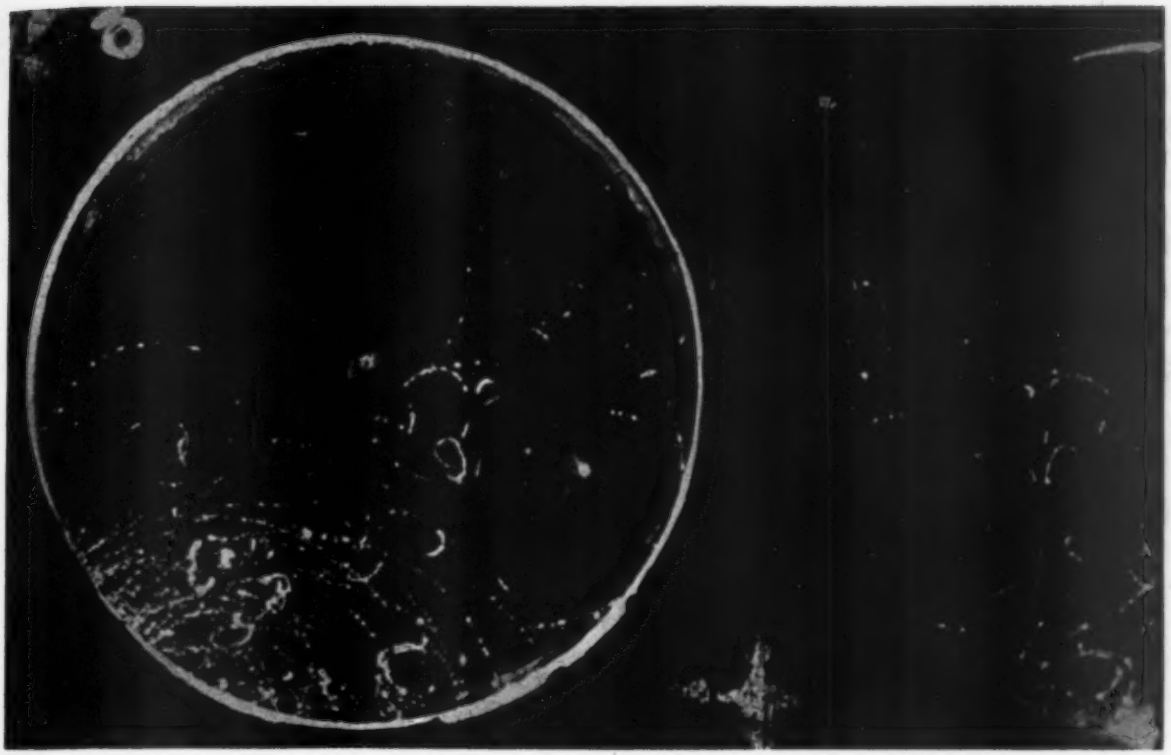

FIG. 2a. Triplet No. 2. Here the triplet origin is near the center of the cloud chamber. Conditions are the same as those in Fig. 1. The triplet is not as nearly coplanar as triplet No. 1 but the calculations on momentum and energy give nearly as good a check as those from triplet No. 1.

lished, it is not clear that there are three particles involved in the event and no data are included to show that momentum is conserved in the process. Groshev[4] looked for triplets while examining the pair produced by RaTh gamma-rays in nitrogen, krypton, and xenon. While observing a total of 435 pairs, no triplets were found. For these reasons the authors wish to report the following data on two triplets which were observed while examining the pairs reported in the preceding paper.

Since the experimental procedure and method of making measurements on the tracks was described fully in the preceding paper it will not be repeated here.

Figures 1 and 2 show photographs of the two triplets which were observed. No conversion foil was used. It is clear from the photographs that all three tracks of the triplets have the same origin in the gas of the cloud chamber.

The experimental data on these triplets, including momentum and energy calculations, are given in Table I.[5] Measurements on the radii of the tracks, of the magnetic field, and the calculation of the electron energies were made according to the procedure described in the preceding paper. The angle that each track of a triplet at its origin makes with the initial direction of the gamma-ray was determined on a photograph of the triplet enlarged to twice life size. To do this the radius of curvature of each track of the triplet on that enlargement was measured with the measuring engine. Then a circle of that radius was drawn in coincidence with the measured track. A line parallel to the direction of the incident gamma-ray was drawn through the origin of the triplet. Now, the angle between a radius constructed from the center of the circle to the vertex of the triplet, and the direction of the incident gamma-ray is comple-

[4] L. V. Groshev, J. Phys. Acad. Sci. U.S.S.R. **5**, 135 (1941).

[5] A preliminary report on these data was given previously. Ogle and Kruger, Phys. Rev. **65**, 61A (1944).

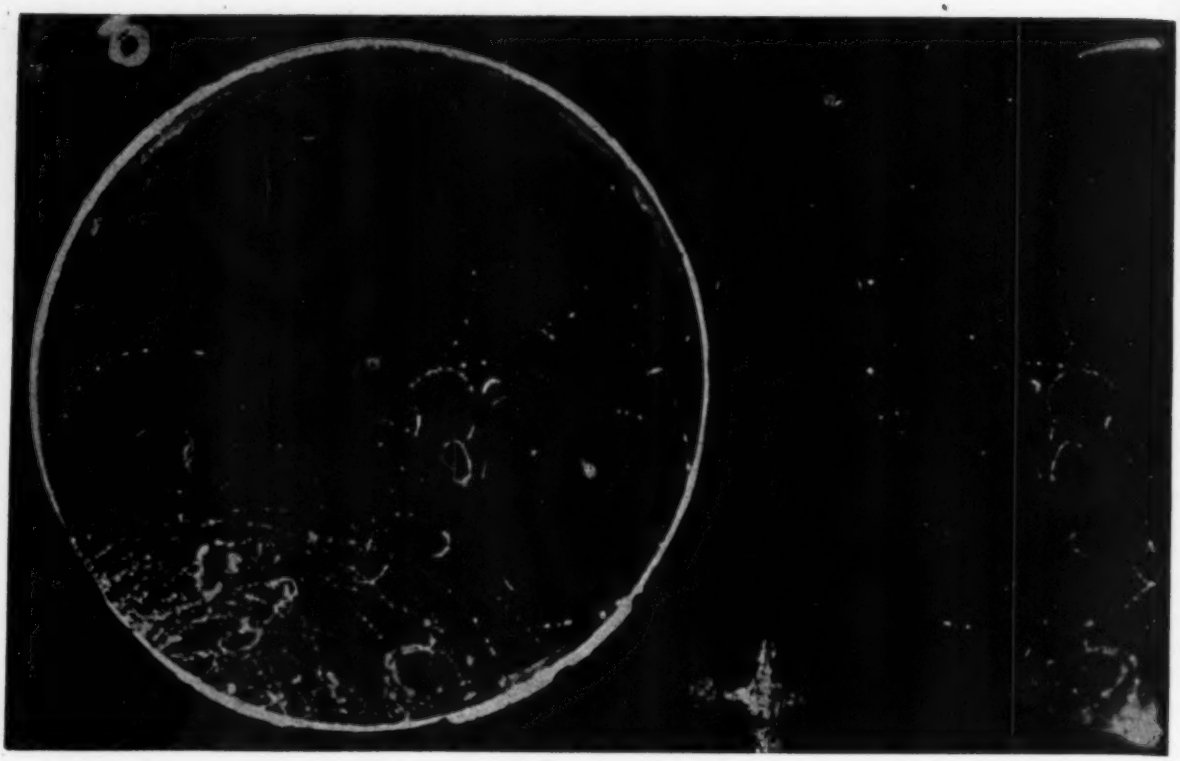

FIG. 2b. Triplet No. 2. Same as Fig. 2a except that several faint droplets near the end of the triplet tracks have been retouched so as to assure good reproduction in the Physical Review.

mentary to the angle between the initial direction of the electron and the direction of the incident gamma-ray. Thus, the initial direction of the electron can be found with an accuracy of about $\pm 2°$.

The energy of the gamma-rays producing

TABLE I. Experimental data on triplets.

ϕ = Initial angle of electron track with respect to the direction of incident gamma-ray.
Hr = Momentum in gauss-cm.
E = Energy in million electron volts.
M = Momentum in g cm/sec. (times 10^{16}).
$h\nu/c$ = Momentum of incident gamma-ray in g cm/sec. ($\times 10^{16}$).
y = the direction of the incident gamma-ray.
x = the direction at right angles to that of the incident gamma-ray.

Data from triplet in Fig. 1

Electron	ϕ	Hr. (Total)	E	Hr_x	Hr_y	M_x	M_y	$h\nu/c$
positron	0°	2613	0.425	0	2613	0	0.414	
electron	−10.2°	4660	0.978	−817	4588	−0.1294	0.726	
electron	26.0°	1924	0.259	842	1729	0.1334	0.274	
sum			1.662	25	8930	0.0040	1.414	1.433
			$2mc^2 = 1.022$					
			2.684 Mev.					

Data from triplet in Fig. 2

positron	8.7°	3566	0.674	523	3525	0.0828	0.558	
electron	3.4°	4388	0.900	260	4380	0.0415	0.693	
electron	−26.5°	898	0.067	−401	804	−0.0635	0.127	
sum			1.641	382	8709	0.0608	1.378	1.422
			$2mc^2 = 1.022$					
			2.663 Mev.					

these triplets, as calculated from these measurements, is 2.68 Mev and 2.66 Mev. This agrees with the 2.68 Mev gamma-ray from $Na^{24} \rightarrow Mg^{24}$ reported in the preceding paper. Momentum relations check well except for the x-component of triplet No. 2. In this case the discrepancy is about 4 percent of the total momentum and represents a not impossible experimental error.

In these studies two triplets were observed while 56 pairs were observed. The probability of ordinary pair production in the field of a nucleus is proportional to Z^2. Since a triplet is formed in the field of an electron the probability of triplet production in an atom should be proportional to Z, the number of electrons present in the atom. Thus the ratio of triplets to ordinary pairs observed should be of the order of $1/Z$. This should hold approximately at high energy but not near the threshold for the processes, since one threshold is at $2\ mc^2$ and the other at $4\ mc^2$. However, if it is assumed that, near the threshold, the shape of the triplet production curve is similar to the pair production curve, the relative probability of the two processes at low energy can be estimated roughly. The pair production probability at 2.7 Mev ($5.3\ mc^2$), as given by Heitler is 0.79 in units of $Z^2r_0^2/137$. $5.3\ mc^2$ is $1.3\ mc^2$ above the threshold for triplet production. The pair probability at $1.3\ mc^2$ above the pair threshold is 0.225 in the same units as above. By assuming that this probability also applies to triplet formation at $1.3\ mc^2$ above the triplet threshold, the ratio of triplet production to pair production is 0.225/0.79 or 1/3.5. Since the triplets and pairs observed were formed in air in a cloud chamber, the above ratio must be reduced by $1/Z$, which for air is about 1/7.2. Thus, the ratio becomes 1/25. The observed ratio of 1/28 is in much better agreement with the estimated ratio than should be expected when so few triplets are observed.

PHYSICAL REVIEW VOLUME 67, NUMBERS 9 AND 10 MAY 1 AND 15, 1945

Atomic Distribution Function of Liquid Argon

C. N. WALL
Department of Physics, University of Minnesota, Minneapolis, Minnesota
(Received March 15, 1945)

An atomic distribution curve for a simple monatomic liquid, such as argon, is generally characterized by a prominent first peak. This peak may be used to determine the elements of the first coordination shell, i.e., the radius of the shell and the number of nearest neighbors of an atom. Frequently this peak can be closely approximated by a simple polynomial involving a parameter σ. This parameter may be determined empirically by a process of fitting. In the case of liquid argon, where the force function between the atoms is known, it is possible to make a theoretical determination of σ provided the elements of the first coordination shell are given. This has been done for liquid argon at a temperature of 91.8°K and under a pressure of 1.8 atmos. The theoretical value of σ is compared with various empirical values obtained from the experimental distribution curve for liquid argon under these conditions as given by Eisenstein and Gingrich. It is found that the theoretical value is somewhat smaller than the empirical value of σ obtained by fitting and slightly larger than that obtained by the Coulson-Rushbrooke method. A possible interpretation of these results is given.

INTRODUCTION

ATOMIC distribution curves for liquid argon over a considerable range of temperatures and pressures have been obtained by Eisenstein and Gingrich[1] by an analysis of x-ray diffraction patterns of the liquid. Previous to this work, Rushbrooke[2] calculated the first peak of the distribution curve for liquid argon at 90°K by use of a general expression for liquid distribution

[1] A. Eisenstein and N. S. Gingrich, Phys. Rev. **62**, 261 (1942).

[2] G. S. Rushbrooke, Proc. Roy. Soc. Edinburgh **60**, 182 (1940); J. G. Kirkwood and E. M. Boggs, J. Chem. Phys. **10**, 394 (1942).

functions derived by Coulson and Rushbrooke[3] and based upon the Lennard-Jones and Devonshire[4] cell model of liquids. In his paper[3] Rushbrooke showed that the polynomial expression given by Wall[5] for a distribution peak was in "quite remarkably close agreement" with his own calculated peak.

A comparison of Rushbrooke's theoretical peak with the Eisenstein and Gingrich experimental peak for liquid argon at approximately the same temperature and density shows that, although the two peaks have about the same shape, there is little agreement as to size and position. This is to be expected since Rushbrooke assumed N_1, the first coordination number, to be 12 as in the solid state, whereas Eisenstein and Gingrich found N_1 to be approximately 7. Also R_1, the radius of the first coordination shell, was taken as 4.077A by Rushbrooke, whereas Eisenstein and Gingrich found $R_1=3.8$A approximately.

It has been found that the polynomial expression closely approximates the first experimental peak for several different liquids.[5,6] It also appears to fit the Rushbrooke theoretical peak for liquid argon. The weakness of the polynomial expression lies in the fact that it involves a parameter σ which, heretofore, has had to be determined empirically. The purpose of this paper is to show how this parameter may be determined theoretically, and to give the results of such determination both for the hypothetical structure of liquid argon used by Rushbrooke and for the observed structure given by Eisenstein and Gingrich.

THEORETICAL DETERMINATION OF σ

The liquid distribution formula for a single peak, e.g., the first, given by Coulson and Rushbrooke[3] is

$$4\pi r\rho_1(r)=\frac{4\pi^2N_1}{R_1v^2}\int_0^\infty r_1e^{-\bar{\phi}/KT}\times\left[2r\psi(\infty)-\int_{|R_1-r_1|}^{|R_1+r_1|}\psi(|r-x|)dx\right]dr_1, \quad (1)$$

where

$$v=4\pi\int_0^\infty s^2e^{-\bar{\phi}/KT}ds, \quad (2)$$

$$\psi(r)=\int_0^r se^{-\bar{\phi}/KT}ds, \quad (3)$$

and N_1 and R_1 are respectively the number of atoms in and the radius of the first coordination shell of atoms. $\rho_1(r)$ is the density of atoms contributed by the first shell and $\bar{\phi}$ is the average potential energy of an atom as a function of its distance s from the center of its cell. For liquid argon $\bar{\phi}(s)$, as given by Lennard-Jones and Devonshire and modified by Corner,[7] is

$$\bar{\phi}(s)=\frac{N_1a}{2s}\left[\frac{\lambda}{(n-2)a^n}\left\{\left(1-\frac{s}{a}\right)^{-n+2}-\left(1+\frac{s}{a}\right)^{-n+2}\right\}-\frac{\mu}{(m-2)a^m}\left\{\left(1-\frac{s}{a}\right)^{-m+2}-\left(1+\frac{s}{a}\right)^{-m+2}\right\}\right]-C, \quad (4)$$

where $a\equiv R_1$, $\lambda=5.43\times10^{-99}$, $\mu=11.1\times10^{-59}$, $n=11.4$, $m=6$, and C is chosen so that $\bar{\phi}(0)=0$. All quantities in Eq. (4) are expressed in c.g.s. units. By use of Eqs. (1)–(4) it is clear that $\rho_1(r)$ may be determined provided N_1 and R_1 are given.

Wall's polynomial expression for $\rho_1(r)$ is a special case of Eq. (1) in which $\bar{\phi}=0$ for $s\leqq\sigma$, and $\bar{\phi}=\infty$ for $s>\sigma$, where σ is an unknown parameter. Equation (1), in this case, reduces to

$$y_1\equiv4\pi r\rho_1(r,\sigma)=\frac{3N_1}{5\sigma R_1}\left\{1-\frac{5(R_1-r)}{4\sigma^2}\times\left[1-\frac{|R_1-r|}{2\sigma}+\frac{|R_1-r|^3}{40\sigma^3}\right]\right\}, \quad (5)$$

for $|R_1-r|\leqq2\sigma$. Outside of this interval $\rho_1(r,\sigma)=0$. From the manner in which σ is defined, it is evident that its determination enables one to make an estimate of the free volume of the liquid. σ may be determined empirically by the process of fitting the right hand member of Eq. (5) to a given experimental liquid distribution peak.

There is, however, a theoretical method of determining σ which does not involve the use of

[3] C. A. Coulson and G. S. Rushbrooke, Phys. Rev. **56**, 1216 (1939).
[4] J. E. Lennard-Jones and A. F. Devonshire, Proc. Roy. Soc. **A163**, 53 (1937); **A165**, 1 (1938).
[5] C. N. Wall, Phys. Rev. **54**, 1062 (1938).
[6] N. S. Gingrich and C. N. Wall, Phys. Rev. **56**, 336 (1939); C. N. Wall, Phys. Rev. **59**, 927A (1941).
[7] J. Corner, Trans. Faraday Soc. **35**, 711 (1939).

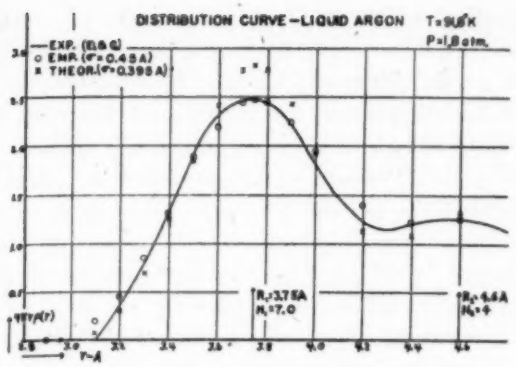

FIG. 1. The experimental distribution curve for liquid argon at a temperature of 91.8°K and a pressure of 1.8 atmos. Empirical and theoretical values of $4\pi r\rho(r)$ for various values of r are also shown for purposes of comparison.

Eq. (5) and which clearly reveals the significance of this parameter. It is evident that the procedure followed in obtaining Eq. (5) from Eq. (1) amounts to replacing the Lennard-Jones and Devonshire potential function for an atom in its cell by the simple but discontinuous function,

$$\bar{\phi}(s,\sigma)=\begin{cases}0 & \text{for } s\leqq\sigma\\ \infty & \text{for } s>\sigma\end{cases}. \tag{6}$$

This function defines a spherical cell of definite radius σ. Its precise relation to the Lennard-Jones and Devonshire function $\bar{\phi}(s)$ given in Eq. (4) is the crux of the matter. It seems reasonable to assume in this case that $\bar{\phi}(s,\sigma)$ must be so chosen that it yields the same average value of s as does the Lennard-Jones and Devonshire function. In other words, the average displacement of an atom from the center of its cell for the two potential functions should be the same. This leads at once to the relation,

$$\tfrac{3}{4}\sigma=\frac{\int_0^\infty s^3 e^{-\bar{\phi}(s)/KT}ds}{\int_0^\infty s^2 e^{-\bar{\phi}/KT}ds}. \tag{7}$$

The left member of Eq. (7) is just the average value of s for $\bar{\phi}(s,\sigma)$ while the right member is that for $\bar{\phi}(s)$. Once the function $\bar{\phi}(s)$ is given, the corresponding value of σ may be determined for any temperature T by means of Eq. (7).

RESULTS

The value of σ has been computed by means of Eqs. (4) and (7) for the case of liquid argon considered by Rushbrooke. The value obtained, *viz.*, $0.140R_1$ compares very favorably with the value, 0.141 R_1, given by Rushbrooke on the basis of matching maxima. This close agreement between the two values of σ makes it worth while to apply this method to another case of liquid argon experimentally studied by Eisenstein and Gingrich.

Distribution curve No. 2 for liquid argon in the paper of Eisenstein and Gingrich[1] was chosen for analysis, first, because the conditions of temperature and density were nearly the same as those postulated by Rushbrooke, and second, because Eisenstein and Gingrich state that they were especially careful in the determination of this curve. The forepart of this curve consisting of the first two peaks is shown in Fig. 1. It should be noted that $y\equiv 4\pi r\rho(r)$ is plotted against r since it is this function, rather than $4\pi r^2\rho(r)$, which is symmetrical about its maxima according to the Lennard-Jones and Devonshire liquid model.[3]

In order to compute σ for this case of liquid argon we make use of Eqs. (4) and (7) with the corresponding values of the constants for argon. The temperature is 91.8°K. The two parameters, N_1 and $R_1\equiv a$, are not given by theory but may be obtained from the experimental curve. We take $N_1=7.0$ and $R_1=3.75$A. The two integrals in Eq. (7) are evaluated by numerical integration by use of the Euler-Maclaurin formula. In this computation $x\equiv s/a$ is used as the argument and the integrands in Eq. (7) are tabulated for values of x running from 0 to 0.25 in steps of 0.01. At $x=0.21$ both integrands become negligibly small. A graph showing $\bar{\phi}/KT$ as a function of x for the state of liquid argon under consideration is given in Fig. 2. The net result of the computation gives a value of σ equal to 0.395A. By inspection of Table I it may be seen that this theoretical value compares very favorably with the various empirical estimates of σ made by direct analysis of the experimental curve.

The four empirical methods of obtaining the values of σ shown in Table I may be described as follows. In method one[5] the right-hand member

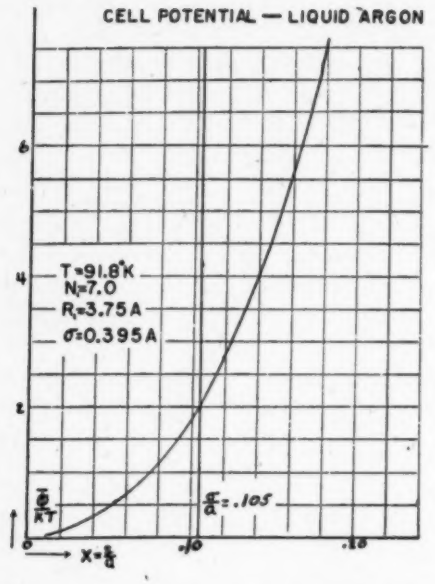

FIG. 2. $\bar{\phi}/KT$ as a function of s/a for liquid argon at a temperature of 91.8°K and a pressure of 1.8 atmos.

of Eq. (5) is fitted to the forepart of the first peak in the experimental curve. In method two[2] the maximum value of y_1, in Eq. (5), i.e., $3N_1/5\sigma R_1$, is made equal to the maximum ordinate of the first peak in the experimental curve. In method three one determines the half-width of the first peak for $y_1 = \frac{11}{12}y_1(\max)$. This half-width just equals σ as is evident by inspection of Eq. (5). Method four, developed by Coulson and Rushbrooke,[3] requires a knowledge of R_1, R_2, $y_1(\max.)$ and $y_2(\max.)$ as well as the density of the liquid. Details of this method are given in their paper.

It will be observed from Table I that the first three empirical methods give values of $\sigma(\leqq 0.45\text{A})$ which are practically identical. It will also be observed from Fig. 1 that this value, when used in Eq. (5), reproduces the experimental curve very well. The theoretical value of $\sigma(=0.395\text{A})$ does not produce such a good fit nor does the empirical value of $\sigma(=0.37\text{A})$ given by method four. It is interesting to note, however, that these latter two values are fairly close together.

Whether or not the differences between the various values of σ are significant is difficult to determine. Perhaps two comments are in order on this score. In the first place, the theoretically computed value of σ is very sensitive to small changes in $R_1 \equiv a$, since high powers of this quantity enter in the expression for $\bar{\phi}(s)$. Also, in computing σ, only the atoms in the first shell are considered. The effect of atoms outside this shell would tend to increase the value of σ slightly but probably not enough to raise its value to 0.45A.

In the second place, it has been tacitly assumed in this work that there exists a definite equilibrium distance R_1 for the atoms in liquid argon corresponding to a definite number of nearest neighbors N_1. This is not likely to be the case. One would certainly expect some spread in the values of R_1 and N_1. If there is a significant spread in values of R_1, then one would expect the first three empirical methods of determining σ to include this spread, whereas the theoretical method and also empirical method four would not include this spread. Hence, one would expect to get somewhat larger values of σ in the former three cases than in the latter two cases, the difference being dependent upon the spread in R_1 values.

TABLE I. σ for liquid argon ($T=91.8$°K, $P=1.8$ atmos.).

Method	σ in A	R_1 in A	y_1 (max.)	N_1	R_2 in A	y_2 (max.)
1 (emp.)	0.45	3.75	2.48			
2 (emp.)	0.45	3.75	2.48	7.0		
3 (emp.)	0.44	3.75	2.48			
4 (emp.)	0.37	3.75	2.48		4.62	1.26
5 (theor.)	0.395	3.75		7.0		

Radioactive Scandium. I*

CARL T. HIBDON,** M. L. POOL, AND J. D. KURBATOV
The Ohio State University, Columbus, Ohio

(Received March 12, 1945)

Sc^{42}: The existence of this radioactive isotope, reported half-life of 13.4 days, has not been confirmed. Sc^{43}: This isotope of 3.92 ± 0.02 hours half-life has been produced by the reactions $Ca(d, n)$, $Ca(\alpha, p)$ and $Ca(p, n)$. Positrons of 1.13 Mev and gamma-rays of 1.65 Mev are emitted. The ratio of the number of positrons to gamma-rays is four. Sc^{44}: One of the isomers of Sc^{44} decays with a half-life of 3.92 ± 0.03 hours. The positrons and gamma-rays have the same energy; namely 1.33 Mev. Three gamma-rays per positron are emitted. Absorption measurements in aluminum and in beryllium indicate characteristic x-rays. The other isomer of Sc^{44} has a half-life of 2.44 days. The genetic relation of the isomers of Sc^{44} has been confirmed.

INTRODUCTION

ARTIFICIAL radioactivity of scandium was first studied by Zyw,[1] who bombarded potassium chloride with alpha-particles of radium *C'* of 55 mm effective range. A half-life period of three hours was found in the scandium fraction. Zyw concluded that the radioactive isotope formed was Sc^{42} or Sc^{44}. No second period was detected. Later Frisch[2] bombarded calcium fluoride with alpha-particles using 600 millicuries of radon as a source of alpha-particles. A half-life period of 4.4 hours, with a possible error of ten percent, was observed in the scandium precipitate. This half-life period was assigned to Sc^{43}. The protons emitted during the bombardment of calcium to form Sc^{43} have been studied by Pollard and Brasefield,[3] who used ThC' as a source of alpha-particles.

Fermi and his co-workers[4] irradiated calcium fluoride in water for 14 hours with a 600-millicurie radon source mixed with beryllium. No activity was observed in the scandium fraction.

Artificial radioactivity of scandium produced by bombarding scandium itself was first studied by von Hevesy,[5] who observed a long half-life period and assigned it to Sc^{46}.

Among the first studies of scandium made with the aid of the cyclotron may be found those resulting from fast neutron bombardments of scandium.[6] The fast neutrons were obtained by bombarding Li with deuterons. Two half-life periods were observed, 4 hours and 2 days, and were assigned to Sc^{43} and Sc^{44}, respectively. A similar investigation was made by Walke.[7]

A later report included three half-life periods in Sc^{46}, namely, 1.1 hours, 85 days and a period greater than one year.[8] A further search was made by Walke[9] for these three periods. Finally the 85-day period remained as Sc^{46}.

A more extensive study of the various radioactive isotopes of scandium was afterwards made by Walke. A survey was carried out to activate K and Ca by alpha-particle bombardments. Calcium and scandium were in turn respectively bombarded with deuterons and with slow and fast neutrons. Some discrepancies were found in the results obtained from the scandium fractions. Later a more complete study was made in which fast neutron bombardments of titanium and vanadium were included. In this final paper, Walke reported the radioactive isotopes of scandium substantially as they were known to exist when the present research was begun.[10]

* Some of these results have been presented at the Columbus meeting of the American Physical Society, April 30 and May 1, 1943.

** Now at Cornell University, Ithaca, New York.

[1] M. Zyw, Nature **134**, 64 (1934).

[2] O. R. Frisch, Nature **136**, 220 (1935).

[3] E. Pollard and C. J. Brasefield, Phys. Rev. **51**, 8 (1937).

[4] E. Fermi *et al.*, Proc. Roy. Soc. **A149**, 522 (1935).

[5] G. von Hevesy, Nature **135**, 1051 (1935).

[6] M. L. Pool, J. M. Cork and R. L. Thornton, Phys. Rev. **52**, 41, 239 (1937).

[7] H. Walke, Phys. Rev. **52**, 777 (1937).

[8] J. M. Cork and R. L. Thornton, Phys. Rev. **53**, 866 (1938).

[9] H. Walke, E. J. Williams and G. R. Evans, Proc. Roy. Soc., **360**, 171 (1939).

[10] H. Walke, Phys. Rev. **57**, 163 (1940).

APPARATUS AND EXPERIMENTAL TECHNIQUES

All bombardments were carried out with the 42-inch cyclotron of The Ohio State University. The bombarding particles used were 20-Mev alpha-particles, 10-Mev deuterons, 5-Mev protons and fast neutrons produced by the (Li+d) reaction. Irradiations continued from 2 to 16 clock hours.

Decay curves were plotted from data secured from measurements on a Wulf unifilar electrometer with an ionization chamber containing freon gas at a gauge pressure of 20 lb. per square inch. Absorption measurements were also made with the aid of this equipment. For the detection of soft radiations, another Wulf unifilar electrometer and ionization chamber were together inverted. A mechanism was used to adjust open samples of radioactive materials very near the aluminum foil which covers the ionization chamber. The foil has a weight of 0.14 mg/cm^2. Therefore, the ionization chamber was necessarily used at atmospheric pressure.

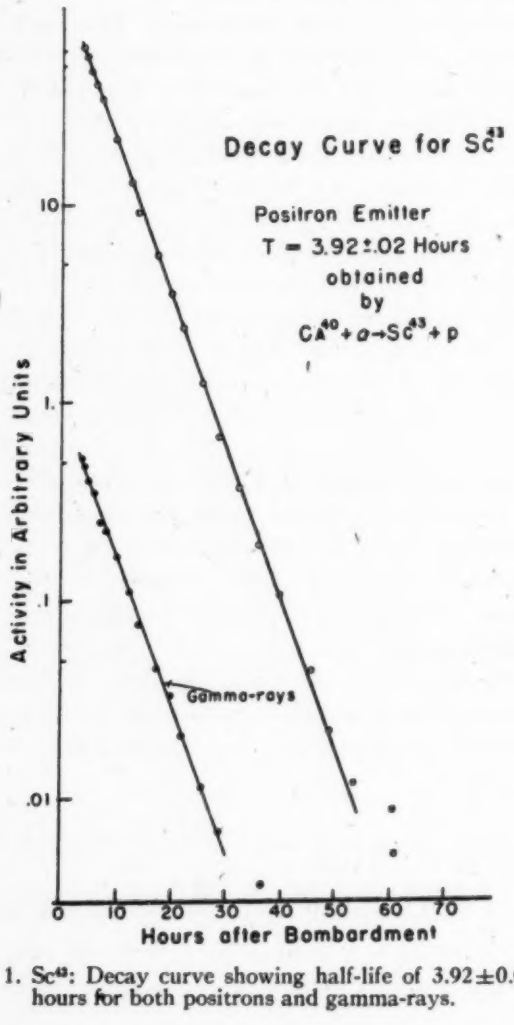

FIG. 1. Sc^{43}: Decay curve showing half-life of 3.92±0.02 hours for both positrons and gamma-rays.

The maximum energy of beta-particles was in most cases found by aluminum absorption measurements. The Sargent formula was used for energies greater than 0.6 Mev and the range-energy relation for energies less than 0.6 Mev.

For the identification of beta-rays a Wilson cloud chamber of 15-cm diameter and a 180° focusing type magnetic spectrometer with a radius of curvature of 16 cm were available.

Gamma-ray energies were measured by absorption in lead and checked by copper and sometimes also by aluminum. A maximum thickness of three inches of lead or of copper was used wherever possible.

In order to obtain the correct absorption coefficient for samples emitting positrons, it was necessary to enclose the sample completely in lead to annihilate all positrons near the sample.

The chemical separations have been made for potassium, calcium and scandium targets. In all cases, the scandium fraction has been separated first by precipitation with oxalic acid and then freed from common impurities by addition of corresponding carriers. The hydrofluoric acid procedure and ammoniacal procedure were employed in purification.

Sc^{42}

A radioactive half-life period of 13.4 days was assigned to Sc^{42} by Walke[10] and was reported to have been produced by the K^{39}(α, n) and Ca^{40}(α, d) reactions. Throughout the present experiments no evidence could be found to indicate the existence of this radioactive period despite repeated efforts to produce and confirm it.

Sc^{43}

A half-life period of scandium varying from 3 to 4.4 hours has often been reported and variously assigned by different experimenters to Sc^{42}, Sc^{43}, or Sc^{44}. The latest assignment was made to Sc^{43} by Walke,[10] who reported a half-life of 4.0±0.1 hours. By aluminum absorption, Walke found two components in the spectrum

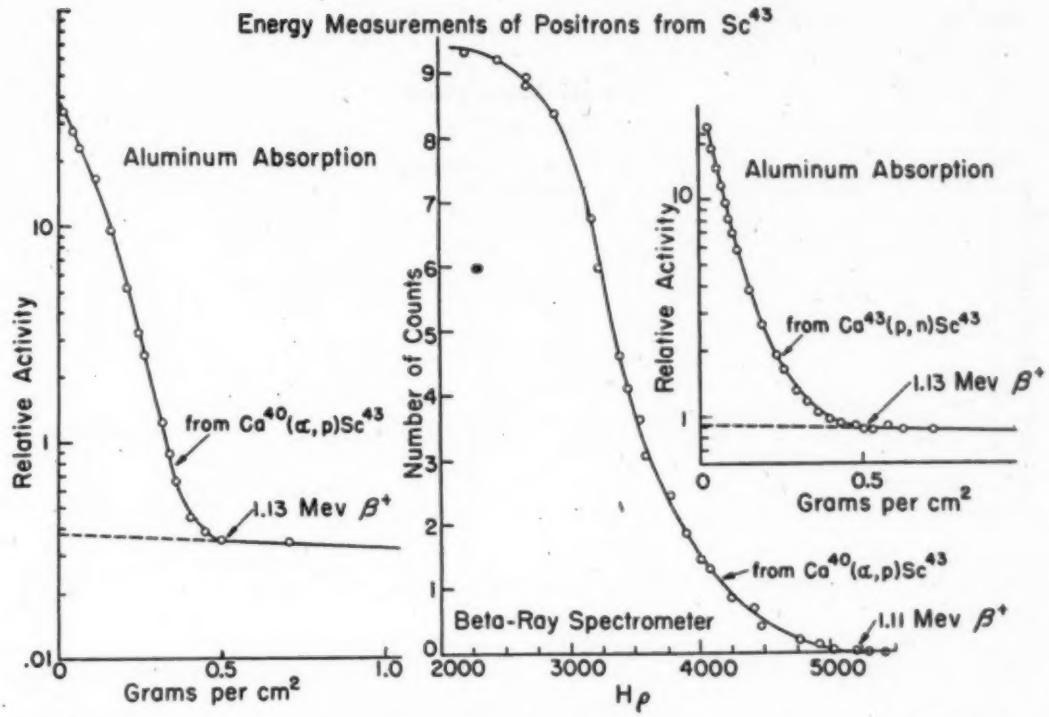

FIG. 2. Sc^{43}: Aluminum absorption and spectrometer measurements of positron spectrum obtained from the $Ca^{40}(\alpha, p)$ and $Ca^{43}(p, n)$ reactions. The end-point is 1.13 Mev.

of Sc^{43} with endpoints at 0.4 Mev and 1.4 Mev (Feather formula). By lead absorption measurements, 1.0 Mev gamma-rays were observed. Sc^{43} was produced by bombarding calcium with deuterons or with alpha-particles.

During the course of the present experiments, Sc^{43} has been rendered extremely active by bombarding calcium with alpha-particles. With this type of bombardment, it is by far the most active isotope of artificially radioactive scandium. Activities ranging up to 30,000 times background have been obtained.

An average half-life of 3.92 ± 0.02 hours was computed from five bombardments. The half-life computed from each bombardment differs very little from this value. A typical decay curve for both the positrons and gamma-rays is shown in Fig. 1.

From aluminum absorption measurements, as shown in Fig. 2, the maximum energy of the positrons was estimated to be 1.13 ± 0.05 Mev (Sargent formula). Measurements made with the magnetic spectrometer indicate a value of 1.11 ± 0.05 Mev.

An energy of 1.65 Mev for the gamma-rays emitted by Sc^{43} has been determined by absorption in lead and in copper. Measurements for lead, as shown in Fig. 3, made with an extremely intense source gave an absorption coefficient of 0.56 cm^{-1}, corresponding to an energy of 1.65 Mev. A very prominent annihilation radiation indicates that more positrons are emitted than 1.65 Mev gamma-rays. From a determination of the ratio of the ionization constant of positrons to that of gamma-rays, it was estimated that one gamma-ray was emitted for every four positrons. The probability that Sc^{43} decays to the ground state of Ca^{43} by positron emission is thus four times that to the excited state by K-electron capture. The presence of x-rays in the difficult region of 3.00A associated with the K-electron capture was not investigated for this isotope.

The detection of the presence of Sc^{43} when produced by proton-bombardment of calcium is complicated by the possible co-production of Sc^{44} and Sc^{48}. However, in the present work the production of Sc^{43} by this type of bombardment has been established as indicated by the half-life, the energy of the positrons and gamma-rays and

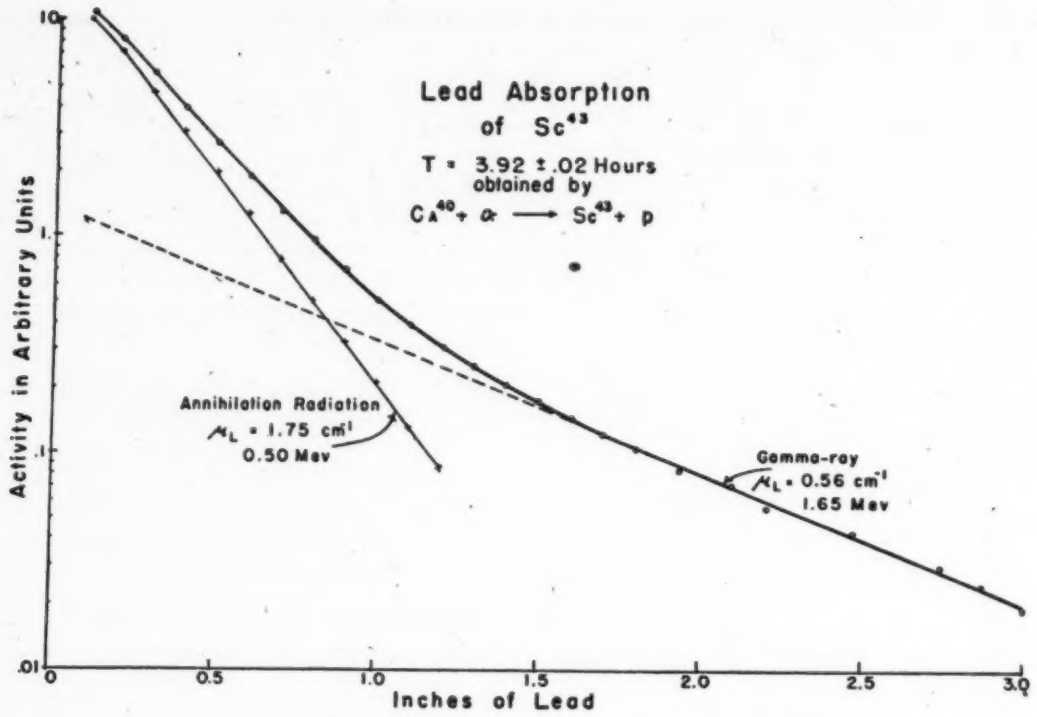

FIG. 3. Sc^{43}: Lead absorption showing gamma-rays of 1.65 Mev.

by the ratio of the intensity of the positrons to that of the gamma-rays.

The detection of the presence of Sc^{43} when produced by deuteron-bombardments of calcium is also complicated by the fact that Sc^{43} and Sc^{44} each have a half-life of 3.92 hours Nevertheless, the presence of Sc^{43} may be established in the presence of Sc^{44} through their respective beta-ray energies of 1.13 and 1.33 Mev and their gamma-ray energies of 1.65 and 1.33 Mev.

THE ISOMERS OF Sc^{44}

As previously reported, Sc^{44} was thought to have genetically related isomers of 4.1- and 52-hour half-lives.[10,11] The 52-hour period (2.16 days) was reported to decay into the 4.1-hour period by the emission of a 0.25 Mev internally converted gamma-ray, and the 4.1-hour period decayed into Ca^{44} by emitting 1.6 Mev positrons.

A restudy of this isotope shows that the scandium fraction of potassium bombarded with

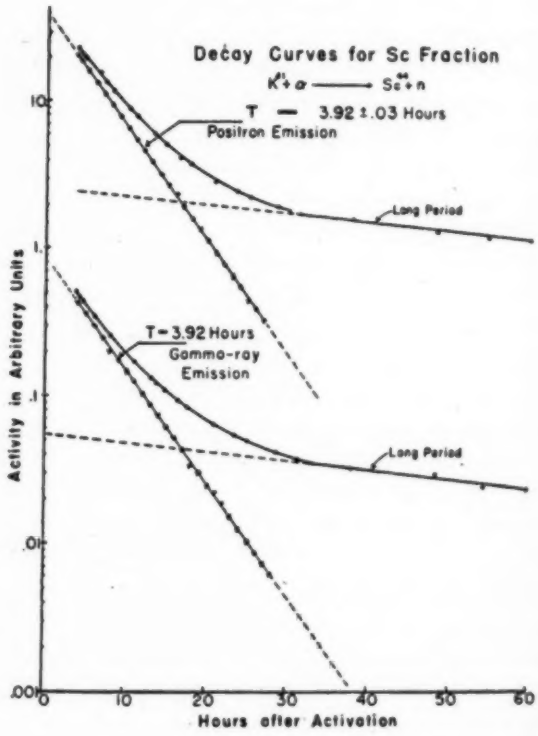

FIG. 4. Sc^{44}: Decay curve showing half-line of 3.92±0.03 hours for both positrons and gamma-rays.

[11] W. E. Burcham, M. Goldhaber and R. D. Hill, Nature **141**, 510 (1938); J. M. Cork and R. L. Thornton, Phys. Rev. **53**, 866 (1938).

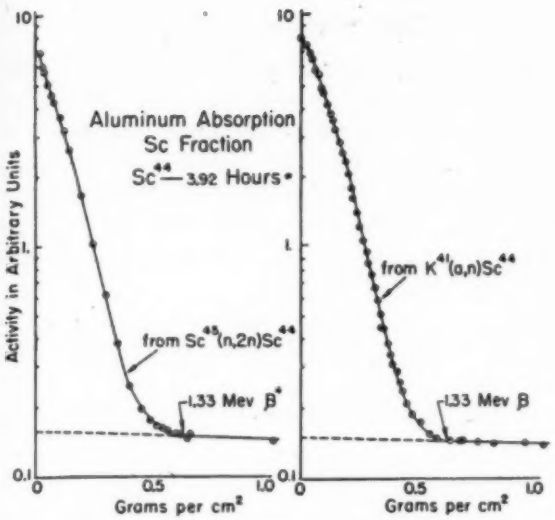

FIG. 5. Sc^{44}: Aluminum absorption measurements of positron spectrum in the 3.92-hour period obtained from the $Sc^{45}(n, 2n)$ and $K^{41}(\alpha, n)$ reactions. The end-point is 1.33 Mev.

alpha-particles yields two main half-life periods, one of 3.92 hours and another of 2.44 days. The same periods were obtained by bombarding scandium with fast neutrons (Li+d). By means of these two bombardments Sc^{44} was obtained free of Sc^{43} and Sc^{48}.

The 3.92-Hour Activity

In Fig. 4 a decay curve is shown for an alpha-particle bombardment of potassium. A very similar curve is obtained for a fast neutron bombardment of Sc. The average half-life obtained from several bombardments was found to be 3.92 ± 0.03 hours in each type of bombardment. The original intensity of the period produced by the $K^{41}(\alpha, n)$ reaction was about 3000 times background while the intensity produced by the $Sc^{45}(n, 2n)$ reaction was only 1000 times background. In each case the subtracted decay curve continued for about seven half-lives.

Aluminum absorption measurements were made at various times during the decay. Typical curves are shown in Fig. 5.

An energy of 1.33 Mev for the gamma-rays has been determined by absorption in lead. Measurements, as shown in Fig. 6 for the $K^{41}(\alpha, n)$ reaction, made with a strong source indicate a small amount of annihilation radiation, and consequently more 1.33 Mev gamma-rays are expected than positrons.

Using the relation between the ionization constants of beta-rays and gamma-rays obtained in the study of Sc^{48}, it was estimated that three gamma-rays are emitted per positron. Absorption measurements in aluminum and in beryllium indicated the presence of x-rays between 2.4 and 2.8A. K-electron capture is therefore strongly indicated.

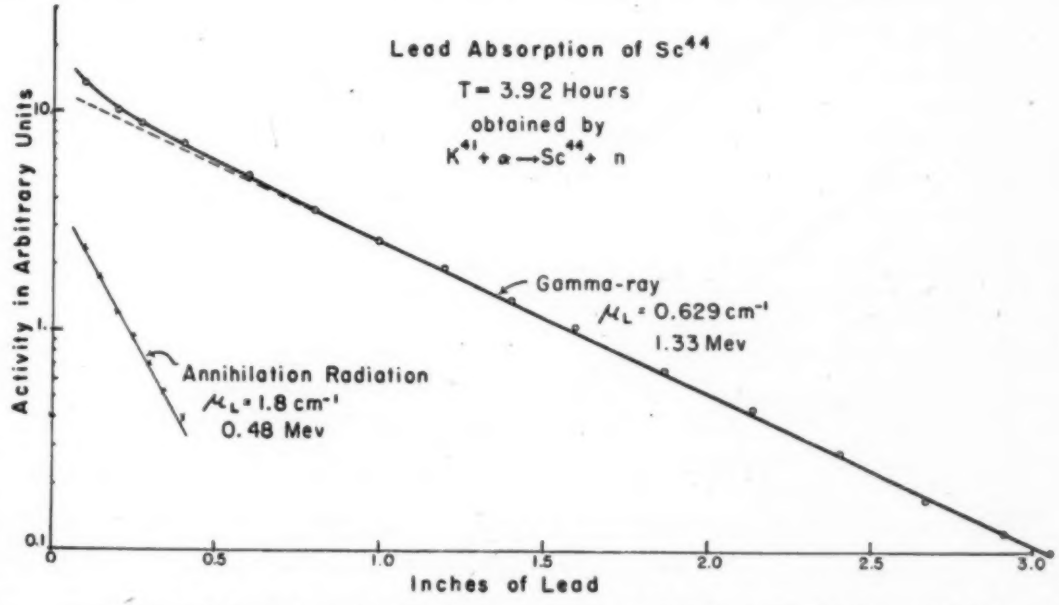

FIG. 6. Sc^{44}: Lead absorption showing gamma-rays of 1.33 Mev in the 3.92-hour period.

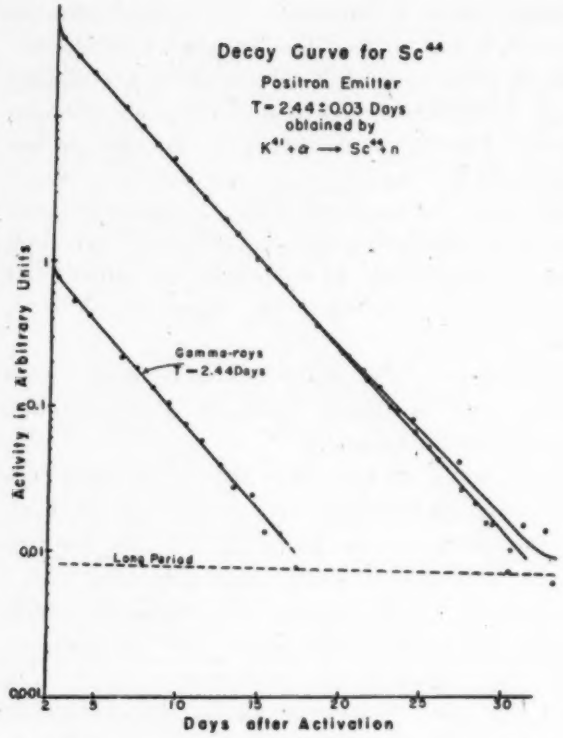

FIG. 7. Sc^{44}: Decay curve showing a half-life of 2.44±0.03 days for both positrons and gamma-rays.

The 2.44-Day Activity

Early during the present work, it was found in bombardments of calcium with deuterons that the gamma-rays of the scandium fraction decayed with a half-life period of 1.83 days rather than with the expected one of 2.16 days.[10] This was reported by Smith[12] and by Mandeville.[13] It remained to be established whether Sc^{44} decayed with a half-life of 2.16 days for the positrons and 1.83 days for the gamma-rays, or whether other radioactive scandium isotopes played an important role.

In order to establish the characteristics of Sc^{44}, it was produced by the reactions $K^{41}(\alpha, n)$ and $Sc^{45}(n, 2n)$. One of the decay curves of the scandium fraction is shown in Fig. 7. From this curve and other similar curves, an average half-life of 2.44 days was observed for both positrons and gamma-rays. The activity could usually be followed for 12 half-lives.

In Fig. 8, similar results are shown for a fast neutron bombardment of scandium. The ratio

[12] Gail P. Smith, Phys. Rev. **61**, 578 (1942).
[13] C. E. Mandeville, Phys. Rev. **62**, 555 (1942); Phys. Rev. **64**, 147 (1943).

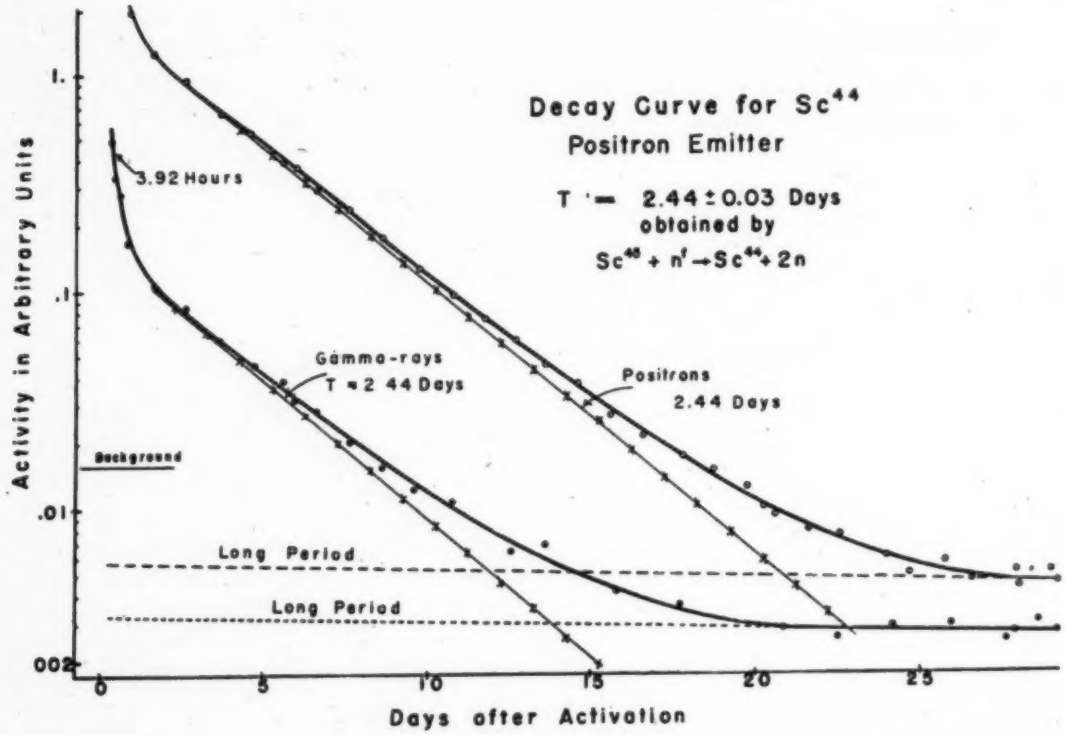

FIG. 8. Sc^{44}: Decay curve showing half-lives of 3.92 hours and 2.44 days for both positrons and gamma-rays obtained by the $Sc^{45}(n, 2n)$ reaction.

of ionizing intensities of the beta-rays to that of the gamma-rays for both bombardments is about 40. This ratio for calcium deuteron bombardments is, however, approximately 15.

From the foregoing data, it therefore appears that deuteron bombardments of calcium produce some other scandium isotope in greater abundance than Sc^{44}. This will be discussed in a later paper.

By aluminum absorption, as indicated in Fig. 9, positrons of maximum energy 1.33 Mev were measured for the $K^{41}(\alpha, n)$ reaction. For comparison the absorption curve for the $Sc^{45}(n, 2n)$ reaction is also included. By absorption measurements made with the inverted electrometer, low energy electrons were observed which are probably due to internally converted gamma-rays of 0.28 Mev energy.

An unconverted gamma-ray was also observed. The energy was 1.33 Mev by absorption in lead, in copper, and in aluminum.

The 1.33 Mev positrons, the 1.33 Mev gamma-ray and the 0.28 Mev internally converted gamma-ray persist throughout the entire decay of the 2.44-day scandium fraction from which it is concluded that the 2.44-day period decays into the 3.92-hour period by emitting the 0.28 Mev gamma-ray. The 1.33 Mev positrons and the 1.33 Mev gamma-rays are, therefore, associated only with the 3.92-hour period.

DuBridge and his co-workers[14] reported the production of the isomers of Sc^{44} by bombardment of calcium with 4 Mev protons. Walke[10] repeated this bombardment with 4 Mev protons and obtained confirmatory results. In the present work no evidence was found to substantiate this reaction although 5 Mev protons were used. However, abundant evidence was found that Sc^{43} was produced.

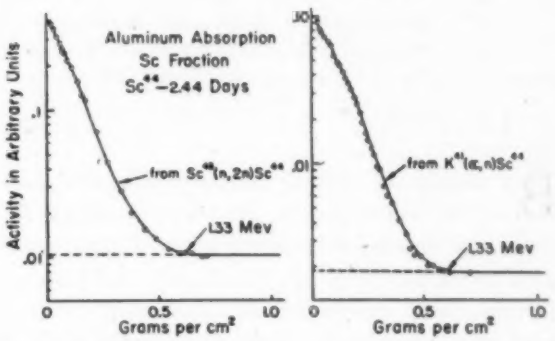

FIG. 9. Sc^{44}: Aluminum absorption measurements of the positron spectrum in the 2.44-day period obtained from the $Sc^{45}(n, 2n)$ and $K^{41}(\alpha, n)$ reactions. The end-point is 1.33 Mev.

ACKNOWLEDGMENT

It is a pleasure to express gratitude for the support received from the University Development Fund and from Mr. Julius F. Stone. Very pure scandium was kindly furnished us by Professor L. L. Quill of Michigan State College. Valuable assistance received through the Graduate School is also acknowledged.

[14] L. A. DuBridge, S. W. Barnes, J. H. Buck and C. V. Strain, Phys. Rev. **53**, 447 (1938).

PHYSICAL REVIEW VOLUME 67, NUMBERS 9 AND 10 MAY 1 AND 15, 1945

The Production of Extremely Short Electromagnetic Waves

JEAN P. COOLEY AND JOHN H. ROHRBAUGH
Washington Square College, New York University, New York, New York
(Received February 10, 1945)

Electromagnetic waves with wave-lengths ranging from approximately 2.2 mm to 0.2 mm were produced. The intensity in the spectra of wire gratings was sufficient to permit absorption measurements to be made. A check of the wave-length assignment was obtained by the use of the first three rotation lines of HI.

BY using as electric dipole radiators many small, aluminum particles in a rapid, continuously flowing stream of oil, radiation measured to be between approximately 2.2 mm and 0.2 mm was produced. The necessary electric field was supplied by a shock excitation circuit generating 1000 surges per second, which were applied to a 1 cm gap containing the oil stream. A steep voltage wave of short duration was required because adequate intensity of radiation could be obtained only by applying to the gap a voltage considerably larger than that required to break down the gap under static conditions. The minimum voltage which produced sufficient intensity of radiation was measured by a 10 cm-sphere gap to be 70 kv, but it is probable that actual instantaneous voltages across the oil stream were much greater. Attempts to determine the actual voltage at the gap with a vacuum tube oscillograph failed because of the short duration of the pulse. The power applied to the gap raised the temperature of the oil only about 1°C during one passage of the oil through the gap. The temperature of the oil was not allowed to rise more than about 5°C above room temperature at any time.

Methods for producing short electric waves similar to those here described have been used with some success by Glagolewa-Arkadiewa[1] and Kalugina.[2] It is interesting to recall that, as early as 1890, Oliver Lodge[3] suggested a technique employing multiple oscillators for the production of radiation. His idea may be regarded as basic in all of the above-mentioned work.

Detection of the radiation was accomplished by using a bismuth-antimony thermopile which had all junctions covered by a coating, 2 mm thick, of 50 percent lampblack and 50 percent tellurium-plated 60-mesh cork dust. A very dilute solution of shellac was used as adhesive and binder. This absorbing material possesses desirable properties of a receiver for short electric waves. It is composed of absorbers of high electrical resistivity having dimensions comparable with the wave-lengths to be received, separated by spaces also comparable with a wave-length, the whole having low thermal capacity per unit volume. The use of a metal such as tellurium for plating the cork particles is suggested by the work of J. E. Ives,[4] who showed that linear absorbers having high electrical resistivity will absorb efficiently a considerable range of wave-lengths. The thermopile output was applied to a shielded Leeds and Northrup Type HS galvanometer, whose deflections were amplified by an optical and electronic amplifier. The amplifying system included a device, essentially feed-back in character, which automatically corrected slow drifts of thermal, optical or electrical origin. The output was read from an integrating galvanometer similar to a fluxmeter in design. The most suitable over-all sensitivity of the detecting system was such that an output indication of one division on the scale corresponded to the absorption of 1.45 (ergs/sec.) per cm² of exposed thermopile surface. In spite of elaborate shielding, coupling between shock circuit and amplifier made it inadvisable to utilize higher amplifications. Actual deflections in the spectrum were of the order of 30 scale divisions.

[1] A. Glagolewa-Arkadiewa, Nature **113**, 640 (1924); Zeits. f. Physik **55**, 234 (1929); Comptes rendus U. R. S. S. **3**, 415 (1934).
[2] A. Kalugina, J. of Exp. and Theor. Phys. U. S. S. R. **9**, 362 (1939).
[3] O. Lodge, Nature **41**, 462 (1890).
[4] J. E. Ives, Phys. Rev. **31**, 185 (1910).

The spectrometer contained off-axis paraboloidal mirrors in careful adjustment which produced a collimated beam 20 cm square. The relative aperture was approximately 1. Transmission gratings were used having elements each of which was composed of a group of thin wires placed side by side so as to simulate a strip. The gratings were coated with lampblack. This construction reduced specular reflection to a minimum. Grating constants were 4.20 mm and 2.10 mm and the slit widths were 70μ and 140μ, respectively, near 600μ. Strong absorption of thermal radiation of short wave-length was obtained by two well separated filters of red selenium on thin pliofilm placed in the optical path. Each was opaque to visible light. With these filters spectrometer response to thermal radiation produced by a red hot solid replacing the source was negligibly small, except in the close vicinity of central image. Data on this type of filter from λ20μ to λ200μ have been published by Seifert and Randall.[5]

In order to check the correctness of the assigned wave-lengths an absorption cell 12 cm thick was used to investigate the region containing the first three rotation lines of HI, which, following Czerny,[6] are known to lie at $\lambda\lambda$779, 389 and 260μ. These values differ, by an amount which is insignificant here, from wave-lengths calculated from the data of Nielson and Nielson.[7] Because of the labor involved with the present form of apparatus no attempt was made to obtain detailed spectral absorption curves of high accuracy. Settings were made on $\lambda\lambda$260, 325, 389, 585, 779 and 1020μ and absorptions of approximately the predicted values were found. The thermal source previously mentioned produced negligible intensity throughout this region. These facts were taken as reasonable proof of the correctness of the wave-length assignments. The spectral energy shows adequate intensity for absorption measurements from approximately λ0.2 mm to the spectrometer limit which was, with the 4.20 mm grating, slightly beyond λ2.2 mm.

[5] H. S. Seifert and H. M. Randall, Rev. Sci. Inst. **11**, 365 (1940).

[6] M. Czerny, Zeits. f. Physik **45**, 476 (1927).

[7] A. H. Nielson and H. H. Nielson, Phys. Rev. **47**, 585 (1935).

An Experimental Determination of the Velocity of Sound in Dry CO_2-Free Air and Methane at Temperatures below the Ice Point

THOMAS HAROLD QUIGLEY, S.J.*
The Johns Hopkins University, Baltimore, Maryland
(Received March 13, 1945)

The fixed path acoustic interferometer has been used for the measurement of the velocity of sound in dry CO_2-free air and in methane between 90°K and the ice point. Acoustic resonance in a limited column of gas, coupled to a driven X-cut quartz crystal of fundamental frequency of about 600 kc per sec., is produced by temperature variation. The procedure is such that differences in temperature readings, when the temperature is rising and when it is falling, are reduced to an amount in keeping with the other errors of measurement. No molecular acoustic dispersion has been observed so that the results are made available with especial reference to their value for computations of specific heats. The results are given, within experimental error, by the formulae: for air, $v^2 = 3.8762\times10^2T + 806 + 1.8043\times10^6T^{-1} - 2.0364\times10^7T^{-2} + 3.007\times10^{-2}T^2$ and for methane, $v^2 = 6.6176\times10^2T + 1.0016\times10^6T^{-1} - 1.3846\times10^8T^{-2}$.

DEVELOPMENTS in ultrasonics in recent years have made it possible to realize the hopes of early students of acoustics and of thermodynamics that the methods of acoustics could be made to yield results of prime importance in the study of gases, especially with reference to their specific heats. Audible sound waves are of such lengths that sound chambers must be either of prohibitive dimensions or such as to introduce boundary effects, considerably complicating the task of finding the specific acoustic properties of the medium.

It is now well known that a characteristic complication in the study of the specific heats of gases by ultrasonics is the possibility of the presence of acoustic dispersion of the molecular type which may be enhanced in some cases by small traces of gaseous impurity. It has been pointed out, however, that the existence of this dispersion may be immediately detected, its amount evaluated, and it may even be avoided by a suitable choice of pressure and frequency ranges in the experiments.[1–3] This point has been well illustrated in the work of Hubbard and Zartman[4] in the development of the fixed path acoustic interferometer as well as by the work of Herget[5] on the velocity of sound in CO_2 and ethylene.

The object of the present work has been twofold: in part, to develop a procedure of maximum precision for sound velocity determinations; and, in part, to apply it to one or more gases of great purity. Air was chosen because of its ready availability for developing the procedure, and methane because the results would be new and because the gas has been studied extensively in spectroscopy. In neither dry CO_2-free air nor in methane at high purity is there any serious question of molecular acoustic dispersion at the frequency used.

The theory of the ultrasonic interferometer, as used here, has been developed in detail in previous publications[6,7] so that it will be sufficient to outline briefly its principal features. A quartz crystal, used as a resonator after the manner of W. G. Cady,[8] is connected across the condenser of a simple wave-meter circuit whose current is measured by a vacuum thermocouple and galvanometer. The wave-meter is tuned close to the frequency of the thickness vibrations of the quartz. When an exciting oscillator is tuned through this frequency, the wave-meter galvanometer will show the usual electrical resonance peak (i^2 *versus* frequency), except that in the immediate neighborhood of the crystal

* Since 1940 Professor of Physics at Holy Cross College, Worcester, Massachusetts.

[1] W. T. Richards and J. A. Reid, J. Chem. Phys. **2**, 193 (1934).
[2] A. H. Hodge, J. Chem. Phys. **5**, 974 (1937).
[3] J. C. Hubbard and A. H. Hodge, J. Chem. Phys. **5**, 978 (1937).
[4] J. C. Hubbard and I. F. Zartman, Rev. Sci. Inst. **10**, 382 (1939).
[5] C. M. Herget, J. Chem. Phys. **8**, 537 (1940).
[6] J. C. Hubbard, Phys. Rev. **38**, 1011 (1931); **41**, 523 (1932).
[7] R. S. Alleman, Phys. Rev. **55**, 87 (1939).
[8] W. G. Cady, Proc. I.R.E. **10**, 83 (1922).

frequency the i^2 readings of the thermocouple-galvanometer system will show a falling away, which, under favorable conditions, will reach near zero values. This is the so-called current *crevasse* associated with the quartz resonator, a phenomenon discovered by Cady.[8] When current readings are a minimum, the crystal is vibrating most vigorously and generating a maximum of back e.m.f. If the crystal is immersed in a fluid of a low density, such as a gas, so as to send out sound waves, such waves will represent energy carried away, and the crevasse will not be so deep. If some of the waves are reflected back to the crystal, they will arrive at some phase so related to the phase of motion of the crystal as to modify the current reading of the crevasse. If the phase of the returned radiation is changed while radiation is taking place, the crevasse reading of minimum i^2 will change, becoming greatest when there is resonance in the medium and smallest at anti-resonance. The maxima occurring at resonance in the gas are called reaction peaks. The length of the sound path (distance from crystal to reflector and back) is an integral number of wave-lengths of sound in the medium at resonance. Thus if v is the sound velocity, f the electrical frequency, λ the wave-length of sound, d the distance from resonator to reflector or $2d$ the length of sound path, and n the number of half wave-lengths in the sound chamber we have: $v=f\lambda=2df/n$.

The fixed path interferometer possesses special advantages for work at low temperatures, there being no moving parts and consequently no necessity for packed joints. Then, too, there is no necessity for a screw or connecting rod passing through a temperature gradient for the communication of motion which has always involved a troublesome correction. The sound chamber of the interferometer developed for the present work consists of a hollow cylinder S (cf. Fig. 1) of fused quartz closed at one end by a plane polished plate R of fused quartz and at the other by the crystal Q which has optically plane and parallel surfaces. The fused quartz cylinder has ends optically plane and parallel so that the length between quartz crystal and reflector can be accurately determined beforehand. This does not appreciably change in the course of the experiment as the coefficient of thermal expansion of quartz is negligibly small. This length, d, was found to be 0.62933 cm. The permanent adjustment to parallelism between crystal source and reflector secured in this way ensures symmetry of reaction peaks and a greater accuracy of determination of half-wave-length spacings than is otherwise possible. The internal diameter of the cylinder was 2.2 cm, outer diameter 3.8 cm. A backing plate and guard ring both at less than $\lambda/4$ from the surface of Q were provided to return unwanted radiation to the crystal.[7]

In the case of the present experiments several possibilities of error should be examined. First, a quartz crystal is by no means a simple linear vibrator. Experience, however, shows that when a crystal yields a crevasse curve showing a sharp response to a single frequency, a fluid medium, bounded on two sides by the crystal and a reflector accurately plane parallel to it, tends at resonance to vibrate in a normal mode yielding results for sound velocity of the highest precision. In the second place, in the present work resonance is secured by varying the temperature of the gas instead of the length of the sound chamber, thereby establishing a correspondence between the temperatures at resonance and the values of n. As is well known, however, the temperature-frequency curve of an X-cut quartz plate shows discontinuities so that, for a given crystal, certain small regions of temperature become unavailable for the production of sound fields. In the present study, the crystal used was so unsatisfactory in the immediate neighborhood of the ice point that no measurements could be taken there. Lastly, the abnormally low coefficients of reflection for ultrasonic waves in gases, first observed by J. C. Hubbard,[6] may be expected to give rise to a second-order correction of the acoustic path length. According to the theory of reflection of sound developed by K. F. Herzfeld,[9] there should be a phase change due to irreversible heat exchange between sound wave and reflector. Alleman[7] has made the necessary adaptation of Herzfeld's theory of reflection to interferometer theory, and, by the assumption that the same phenomenon of dissipative loss occurs on emission as on reflection,

[9] K. F. Herzfeld, Phys. Rev. **53**, 899 (1938).

has found agreement between the predictions of Herzfeld's theory and the results of measurement of reflection coefficients by the interferometric method. A calculation of the effective change of path length owing to phase change on reflection in the present experiments shows it to be insignificant.

The measurement of the velocity of sound by the present method is thus reduced to the measurement of the length of the sound chamber (which in the present work was determined to better than one part in ten thousand); to the measurement of frequency (again, known to about one part in ten thousand); to the determination of the integral number of half wavelengths (uniquely determined), and finally to the measurement of the temperatures of the gas at the times of reaching reaction peaks.

A schematic diagram of the lower section of the cryostat and enclosed interferometer is given in Fig. 1. The cryostat was placed in a Dewar flask (omitted from the diagram) about 53 cm in length and extended from the bottom of the Dewar to a point slightly higher than its opening where it was held in position and supported by a wooden collar which was part of the cover of the wooden box enclosing the flask. This outer box was packed with cotton waste to insulate the flask from the temperature of the room. The cryostat consisted of a long double-walled pyrex glass tube. The outer wall was joined to the inner one by a ring seal near the point where the cryostat reached out of the Dewar flask. The top of the double-walled glass tube was closed by a ground glass stopper, which supported the nickel-silver tubing *N* and the attached assembly described in Fig. 1.

A thin film of gold was evaporated upon the top surface of the hollow fused quartz cylinder *S*: in part to make electrical contact with the bottom electrode on the face of the resonator, and in part to make connection with an outside lead (not shown). Thin brass rods, inserted in slots cut into the sides of the reflector and cylinder near the outer diameter served to hold the unit together. Gentle pressure supplied by light springs under nuts on the rods secured close contact between reflector and cylinder and ensured constancy of length of the sound chamber. Electrical contact was made by strips

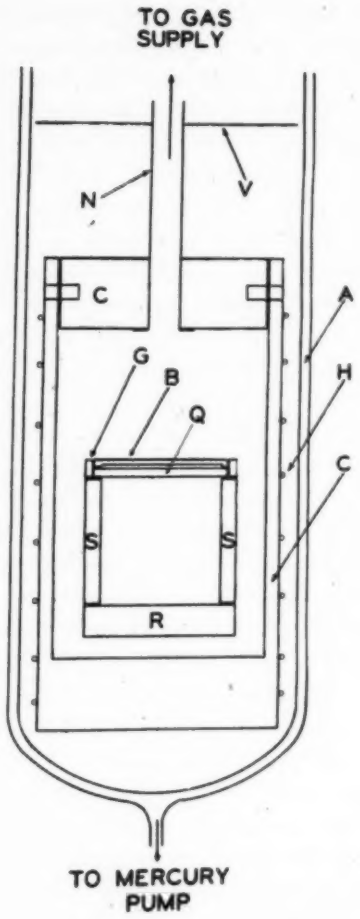

FIG. 1. Details of apparatus. Interferometer chamber, consisting of hollow cylinder *S* and reflecting plate *R*, both of fused quartz, the crystal resonator *Q* with soapstone guard ring *G* and brass backing plate *B*. A copper wire lead (not shown) connects backing plate to wave meter circuit. The fused quartz cylinder has inside diameter 2.2 cm, outside diameter 3.8 cm, height 0.62933 cm. This is the value of *d* (one-half "sound path"). The thickness frequency of resonator is about 587 kc/sec.

Cryostat and temperature control. Air space *A* between walls of cryostat to control by variation of low pressure, heat flow from inside cryostat to liquid nitrogen outside in Dewar flask (not shown); nichrome heating coil *H* wound on copper heat distributor *C*. Aluminum vanes *V* to reduce convection and radiation supported by nickel-silver tube *N*. Electrical leads not shown in the diagram.

of tin foil, mechanically held in place, between the film of gold on an exposed part of the top of the quartz cylinder and one of the brass rods. This brass rod was connected to one of the leads going to the wave-meter circuit.

The temperature of the interferometer unit was measured by a copper-constantan thermocouple (omitted from Fig. 1) soldered to the inside of the copper cylinder *C*; the leads were

brought outside through the nickel-silver tubing *N*. The Copper-Constantan Thermocouple Reference Tables by Southard and Andrews[10] were used for converting from thermal e.m.f. to degrees Kelvin; a correction curve being obtained from the boiling point of oxygen, the freezing point of mercury and the ice point.

The chief difficulty in the measurements was encountered in the determination of the temperature of the gas in the sound chamber when the reaction peak reached its maximum. Since the reaction peaks themselves were very sharp, there was little difficulty in picking the maximum with precision. The determination of the temperature proved to be, as was to be expected, the limiting factor in the accuracy of the work.

Strictly speaking, the temperature measured was that of the copper cylinder *C*, while what was desired was the temperature of the gas within the interferometer. By trial and error it was found necessary to change the temperature not faster than two degrees per hour and in the region of the reaction peaks even more slowly.

TABLE I. Dry CO_2-free air. (Atmospheric pressure.)

n equals the number of half-wave-lengths in the sound chamber.
T equals the absolute temperature (taking 0°C, as equal to 273.1°K).
Δv^2 equals the deviation of the square of the observed value of the velocity from the value of v^2 computed from the empirical equation.

n	T	Frequency (kc/sec.)	Velocity (meters/sec.)	$v^2(10^{-4})$	Δv^2
23*	258.46	587.42	321.46	10.3337	22
23	258.57	587.52	321.56	10.3369	34
24*	237.64	587.73	308.23	9.5006	−22
24	237.66	587.73	308.23	9.5006	−14
24	237.69	587.62	308.17	9.4969	35
25*	219.05	587.88	295.97	8.7598	−74
25	219.30	587.88	295.97	8.7598	26
25	219.24	587.80	295.94	8.7580	19
26	202.88	588.05	284.68	8.1043	3
26	202.98	587.93	284.62	8.1009	77
27	188.21	588.16	274.19	7.5180	−4
27	188.21	588.20	274.20	7.5186	−9
28	175.19	588.22	264.42	6.9918	−49
29*	163.21	588.27	255.32	6.5188	−7
29*	163.14	588.21	255.29	6.5173	−22
30*	152.14	588.42	246.87	6.0945	−196
31*	142.33	588.44	238.92	5.7083	−168
32*	134.23	588.52	231.48	5.3583	−23
33*	126.64	588.54	224.48	5.0391	108
33	126.99	588.50	224.47	5.0387	254
34*	119.03	588.59	217.89	4.7476	−59
34*	119.05	588.62	217.90	4.7480	−55
34	119.89	588.56	217.87	4.7467	285
35*	112.49	588.62	211.63	4.4787	−34
36*	106.43	588.64	205.80	4.2354	−88
37*	100.95	588.67	200.25	4.0100	−101
38*	96.06	588.67	194.99	3.8021	−63
39*	91.74	588.69	189.98	3.6092	43
39	91.83	588.69	189.98	3.6092	80

* Indicates that reading was taken in a run with the temperature decreasing.

Empirical equation for dry CO_2-free air:

$$v^2 = 3.8762(10^2)T + 806 + 1.8043(10^5)T^{-1} - 2.0364(10^7)T^{-2} + 3.007(10^{-5})T^2.$$

[10] J. C. Southard and D. H. Andrews, J. Frank. Inst. **207**, 323 (1929).

TABLE II. Methane. (Atmospheric pressure.)

n is the number of half-wave-lengths in the sound chamber.
T is the absolute temperature (0°C = 273.1°K).
Δv^2 is the deviation of the square of the experimental value of the velocity of sound from the value of v^2 computed from the empirical equation.

n	T	Frequency (kc/sec.)	Velocity (meters/sec.)	$v^2(10^{-4})$	Δv^2
18*	252.54	587.53	410.83	16.878	14
18	252.85	587.53	410.83	16.878	34
18	253.10	587.44	410.76	16.872	56
19*	226.09	587.91	389.45	15.167	−33
19*	225.74	587.75	389.35	15.159	−49
19	226.47	587.75	389.35	15.159	0
19	226.05	587.77	389.37	15.161	−30
20	203.53	587.96	370.02	13.692	−64
21*	186.62	588.16	352.53	12.428	61
21	186.30	588.20	352.55	12.429	38
21	184.80	588.11	352.49	12.425	−59
22*	170.34	588.31	336.59	11.329	54
22	168.62	588.24	336.55	11.327	−61
23	154.77	588.34	321.97	10.367	−55
24*	144.18	588.45	308.61	9.524	46
24	144.26	588.36	308.56	9.521	55
25*	133.55	588.50	296.29	8.779	33
26*	124.21	588.54	284.91	8.117	11
27*	115.58	588.62	274.40	7.530	−51

* Indicates that the reading was taken in a run with the temperature decreasing.

Empirical equation for methane:

$$v^2 = 6.6176(10^2)T + 1.0016(10^4)T^{-1} - 1.3846(10^5)T^{-2}.$$

It was not difficult to obtain a good estimate of the lag of the temperature of the gas behind that of the copper cylinder by changing the rate of heating or cooling as the bottom of the crevasse started to rise. In many instances, the temperature change in passing through the half-width of the reaction peak was less than one degree, and consequently changes in temperature in the sound field of the order of a thousandth of a degree could easily be detected when readings were taken along the steep slope of the reaction peak. If, when a change of pace in heating (or cooling) was introduced, the temperature of the copper cylinder (as given by the potentiometer) remained practically stationary, while at the same time the bottom of the crevasse continued slowly to rise, then equilibrium would be awaited: and if the lag was so great that the reaction peak was passed, the reading was discarded. Equilibrium to within the desired limit of experimental error between the temperature

of the copper cylinder and that of the gas in the sound field at the temperatures for the maxima of the reaction peaks was secured by spending one to several hours in slowing traversing the half-width of the reaction peaks.

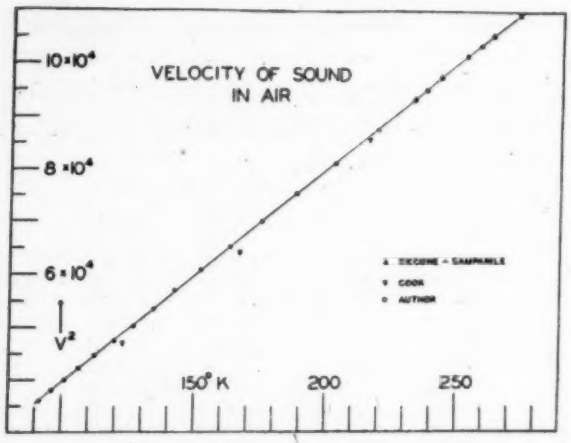

FIG. 2. Graph of velocity of sound in air at atmospheric pressure. Ordinate scale for v^2 in (m/sec.)^2.

The external gas circuit was made of Pyrex glass tubing leading from the gas supply to a Torricelli pump for maintaining the gas at the desired pressure (in the present work, at atmospheric pressure). It then extended to a manometer, a trap, an outlet to an oil pump for evacuating the assembly, then to a mercury safety valve, and finally to the nickel-silver tubing by a short length of rubber pressure tube just long enough to enable the glass stopper and the connected assembly to be removed from the cryostat.

A Dow electron-coupled oscillator, with two stages of amplification, provided an e.m.f. of constant amplitude and frequency for driving the quartz resonator. The output of the second stage of amplification was loosely coupled to the inductance coil of a wave-meter circuit containing, besides the coil, a variable condenser and vacuum thermocouple. The interferometer leads were connected across the variable condenser, and the current in the wave-meter circuit was read from a wall galvanometer connected to the thermocouple.

The electrical frequency was determined by beating the oscillator frequency against the carrier frequency of nearby broadcast stations. A rough calculation from a previously made determination of the velocity of sound at 0°C made it possible to determine uniquely the number of half-wave-lengths in the chamber at the first reaction peak encountered with decreasing temperature. From then on, it was simply a matter of counting.

The results for air and methane are given in Tables I and II, respectively. An empirical equation in each case was found by the method of least squares. The empirical equations are plotted in Figs. 2 and 3, and the experimental readings are indicated by circles. Where two or more readings were too close for separate plotting, the reading of greatest deviation from the curve is given in the figure. In conformity with the tables of Southard and Andrews,[10] 0°C is taken as equal to 273.1°K.

Two other sets of readings are plotted in Fig. 2. Ciccone and Campanile[11] made measurements for each degree from −40°C to 60°C. Their points are in good agreement with the curve. S. R. Cook[12] made several measurements for temperatures throughout the range of the curve. The readings made by Cook in his second series of measurements are found all to lie below the curve. Extrapolating the curve to the ice point gives for the velocity of sound in dry CO_2-free air at 0°C the value 330.6 m/sec. This is lower than the value given by the International

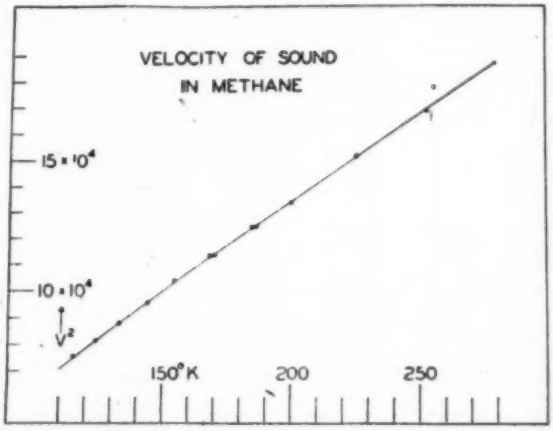

FIG. 3. Graph of velocity of sound in methane at atmospheric pressure. Ordinate scale for v^2 in (m/sec.)^2.

Critical Tables, namely 331.45 m/sec. and that given by Kneser,[13] 331.6 m/sec.

[11] L. Ciccone and F. Campanile, Rend. di Napoli **5**, 187 (1891).
[12] S. R. Cook, Phys. Rev. **23**, 212 (1906).
[13] H. O. Kneser, Ann. d. Physik **34**, 665 (1939).

Extrapolating the curve in Fig. 3 to the ice point gives for the velocity of sound in methane the value 427.2 m/sec. This is lower than the value 429.2 m/sec. given by Dixon, Campbell, and Parker.[14]

The present design could be improved by admitting the gas through a labyrinth in the wall of the copper cylinder and by reading the temperature of the gas from a resistance thermometer wound in a very thin fused quartz ring fitting snugly within the hollow cylinder of fused quartz, thereby securing greater accuracy in temperature measurement and reducing the temperature lag.

The author expresses his gratitude to Professor J. C. Hubbard for suggesting the subject of the research and for his constant encouragement and guidance throughout the work; to Dr. E. R. Blanchard for advice in designing the cryostat; and to Dr. F. O. Rice, of the Catholic University of America, for suggesting the choice of methane and supplying a sufficient quantity purified by the Podbielniak apparatus.

[14] H. Dixon, O. Campbell, and A. Parker, Proc. Roy. Soc. Lond. **100**, 1 (1921).

PHYSICAL REVIEW VOLUME 67, NUMBERS 9 AND 10 MAY 1 AND 15, 1945

Approximate Solutions of the Integral Equations in Scattering Problems

C. F. HSÜEH AND S. T. MA
National University of Peking, Kunming, China

(Received March 10, 1945)

In view of the difficulty of solving exactly the integral equations in the quantum theory of scattering in which radiation damping is taken into account, an approximate method of solution is proposed.

THE investigation of the influence of radiation damping on scattering processes in quantum theory by Waller,[1] Heitler,[2] Wilson,[3] Peng,[2] and others is a very important improvement on the old theory of scattering in which the radiation damping is neglected, both from the theoretical point of view and for interpretation of experimental results. The new theory, however, gives rise to some technical difficulty. The mathematical treatment of the radiation damping in quantum theory involves integral equations. Except in very few cases, the integral equations are so complicated that they cannot be solved exactly. In order to obtain solutions which give essentially correct results, one has often to simplify the problems by neglecting some features of the problems which are comparatively less important, such as transition to negative energy states, the recoil of the heavy particle, or the angular distribution of the scattered particle. Such approximate treatments are necessary for practical purposes. Owing to the approximations thus introduced, however, the results are somewhat less certain than in the old theory. In view of this difficulty, it is desirable for checking the results to find approximate solutions by various independent methods. The results obtained would be more reliable provided they are in reasonable agreement with one another.

One approximate method which enables us to retain all the physical features of the processes but make approximations in the mathematical treatment is the following. In the notation of our previous works[4] the function U_{fi} which determines the transition from an initial state i to a final state f is

[1] Waller, Zeits. f. Physik **88**, 436 (1934).
[2] Heitler, Proc. Camb. Phil. Soc. **37**, 291 (1941); Heitler and Peng, Proc. Camb. Phil. Soc. **38**, 296 (1942); Hamilton, Heitler, and Peng, Phys. Rev. **64**, 78 (1943).
[3] Wilson, Proc. Camb. Phil. Soc., **37**, 301 (1941).
[4] Ma and Hsüeh, communicated to the Proceedings of the Cambridge Philosophical Society.

determined by the integral equation

$$U_{fi}=H_{fi}-i\pi\sum_{p_{f'}}\int H_{ff'}U_{f'}\rho_{f'}d\Omega_{f'}. \tag{1}$$

This equation is closely related to the equation

$$\sum_{p_i}\sum_{p_f}\int\delta U^*_{fi}\left[U_{fi}-H_{fi}+i\pi\sum_{p_{f'}}\int H_{ff'}U_{f'}\rho_{f'}d\Omega_{f'}\right]\rho_f d\Omega_f=0, \tag{2}$$

where δU^*_{fi} denotes an arbitrary variation of the complex conjugate of U_{fi}. For, if (1) is satisfied by a certain function U_{fi} and this solution is substituted in the left-hand side of (2), (2) will be satisfied for any arbitrary variation of U^*_{fi}. On the other hand, if the variation of U^*_{fi} is entirely arbitrary, (2) will obviously lead to (1). The two equations are therefore equivalent to each other. The second equation, however, provides us with the following approximate method for solving (1).

An approximate solution can be obtained by assuming U_{fi} to be some known function which involves some unknown parameters. On substituting this function in (2) and varying the parameters of U^*_{fi}, we obtain a system of algebraic equations from which the numerical values of the parameters can be determined. By increasing the number of parameters we can make the approximate solution approach the exact solution as closely as required. If the function for the approximate solution is suitably chosen, it is possible that we can obtain fairly good results with only a few parameters. This method is similar to the variational method often used in atomic physics.

A simple approximate solution is

$$U_{fi}=xH_{fi}, \tag{3}$$

where x is a parameter independent of f and i. For low energies, the second term on the right-hand side of (1) is negligible and consequently the exact solution is just the expression (3) with $x=1$. As the energy is increased, U_{fi} becomes more and more different from H_{fi}, but the change of the parameter x will partially represent the departure of U_{fi} from H_{fi}. We may therefore expect (3) to give a scattering cross section not much different from the exact one.

On substituting from (3) in (2) and varying U^*_{fi}, we find

$$\delta x^*\sum_{p_i}\sum_{p_f}\int H_{if}\left[H_{fi}(x-1)+i\pi x\sum_{p_{f'}}\int H_{ff'}H_{f'i}\rho_{f'}d\Omega_{f'}\right]\rho_f d\Omega_f=0. \tag{4}$$

Solving for x we obtain

$$x=a/(a+ib), \tag{5}$$

where

$$a=\sum_{p_i}\sum_{p_f}\int H_{if}H_{fi}\rho_f d\Omega_f,\quad b=\pi\sum_{p_i}\sum_{p_f}\sum_{p_{f'}}\int\int H_{if}H_{ff'}H_{f'i}\rho_f\rho_{f'}d\Omega_f d\Omega_{f'}. \tag{6}$$

If we denote by $d\phi_0$ the differential cross section given by the theory in which radiation damping is neglected and by $d\phi'$ the differential cross section given by the new theory corresponding to the approximate solution (3), we have

$$d\phi'=d\phi_0|x|^2=d\phi_0/[1+(b^2/a^2)]. \tag{7}$$

This result is of the same form as a formula previously given by Wilson,[3] but the damping factors in the two formulae are different.

A simple test of (3) and (7) is provided by the non-relativistic scattering of a light quantum by an electron at rest, for which the exact solution is known. Using Wilson's notation, we have

$$H_{fi}=(e^2/2\pi mchk)e\cdot e_0,\quad H_{ff'}=(e^2/2\pi mchk)e\cdot e',\quad \rho_f=k^2/c.$$

Consequently by (6)

$$a=(e^2/2\pi mchk)^2(k^2/c)\sum_{e_0}\sum_{e}\int(e_0\cdot e)(e\cdot e_0)d\Omega_f,$$

$$b=\pi(e^2/2\pi mchk)^3(k^2/c)^2\sum_{e_0}\sum_{e}\sum_{e'}\int\int(e_0\cdot e)(e\cdot e')(e'\cdot e_0)d\Omega_f d\Omega_{f'}, \tag{8}$$

so that

$$b/a=\pi(e^2/2\pi mchk)(k^2/c)(8\pi/3)=(4\pi/3)(e^2/mc^2)(v/c).$$

It follows therefore from (5), (3) that

$$U_{fi}=(e^2/2\pi mchk)e\cdot e_0(1+i(4\pi/3)(e^2/mc^2)(v/c))^{-1}. \tag{9}$$

This result is in complete agreement with the exact solution.

Another test of our approximate formula is provided by the scattering of a positive meson by a neutron or a negative meson by a proton, for which exact solution can be easily found owing to the degeneracy of the nucleus of the integral equation. Each of these processes takes place in two successive stages through some intermediate states which we denote by n, n', n''. It follows therefore from (6) that

$$a=\sum_{p_i}\sum_{p_f}\sum_{p_n}\sum_{p_{n'}}\int\frac{H_{in}H_{nf}H_{fn'}H_{n'i}}{(E_i-E_n)(E_i-E_{n'})}\rho_f d\Omega_f,$$

$$b=\pi\sum_{p_i}\sum_{p_f}\sum_{p_{f'}}\sum_{p_n}\sum_{p_{n'}}\sum_{p_{n''}}\int\int\frac{H_{in}H_{nf}H_{fn'}H_{n'f'}H_{f'n''}H_{n''i}}{(E_i-E_n)(E_i-E_{n'})(E_i-E_{n''})}\rho_f\rho_{f'}d\Omega_f d\Omega_{f'}. \tag{10}$$

For the scattering of a positive meson by a neutron in the frame of reference in which the momenta of the two particles are equal and opposite, we have, in the notation of our previous papers,[4]

$$H_{ni}=v_n{}^P(0)\dagger\xi\dagger v_i{}^N(-p_0)(1-ip_0\cdot\beta/mc)\beta_4{}^2u_i(p_0),$$

$$H_{fn}=u_f(p)\dagger\beta_4{}^2(1+ip\cdot\beta/mc)v_f{}^N(-p)\dagger\xi\dagger v_n{}^P(0),$$

$$\rho_f=pEE_N/c^2h^3E_i.$$

The quantities a and b are found by substituting these expressions in (10) and proceeding in the same way as in the evaluation of scattering cross sections in the theory in which radiation damping is neglected. The calcuulation is straightforward but rather lengthy. The result is

$$a=\rho_f\left[\frac{2\pi h^2c^2}{EE_N(E_i^2-M^2c^4)}\right]^2\int[(AE_i+BMc^2)^2+(BE_i+AMc^2)^2+C^2(E_i^2-M^2c^4)\cos\theta_{fi}]d\Omega_f,$$

$$b=\pi\rho_f{}^2\left[\frac{2\pi h^2c^2}{EE_N(E_i^2-M^2c^4)}\right]^3\frac{AE_i+BMc^2}{2}\int\int[(AE_i+BMc^2)^2+3(BE_i+AMc^2)^2$$
$$+C^2(E_i^2-M^2c^4)(\cos\theta_{fi}+\cos\theta_{f'i}+\cos\theta_{ff'})]d\Omega_f d\Omega_{f'},$$

where we denote by θ_{fi}, $\theta_{f'i}$, $\theta_{ff'}$ the angles through which the meson is scattered. On integrating over all angles we find

$$a=4\pi\rho_f\left[\frac{2\pi h^2c^2}{EE_N(E_i^2-M^2c^4)}\right]^2[(AE_i+BMc^2)^2+(BE_i^2+AMc^2)^2],$$

$$b=16\pi^3\rho_f{}^2\left[\frac{2\pi h^2c^2}{EE_N(E_i^2-M^2c^4)}\right]^3\frac{AE_i+BMc^2}{2}[(AE_i+BMc^2)^2+3(BE_i+AMc^2)^2]. \tag{11}$$

Substituting these results and

$$d\phi_0=\frac{1}{b}\frac{1}{E_i^2(E_i^2-M^2c^4)^2}[(AE_i+BMc^2)^2+(BE_i+AMc^2)^2+C^2(E_i^2-M^2c^4)\cos\theta_{fi}]d\Omega_f,$$

in (7), we obtain the approximate differential cross section $d\phi'$. The total cross section ϕ' is then obtained by integrating over all directions of the scattered meson.

The agreement between the cross section ϕ' thus obtained and that calculated from the exact formula of our previous works, which we denote by ϕ, is fairly good, as shown in Table I for the scattering of vector mesons.

An approximate solution slightly better than (3) is

$$U_{fi}=H_{fi}(x+ye^{i\theta_{fi}}), \tag{12}$$

where x and y denote two parameters independent of i and f. We obtain now from (2), on varying x^* and y^* independently,

$$\begin{aligned}&\delta x^*\sum_{p_i}\sum_{p_f}\int H_{if}\left[H_{fi}(x+ye^{i\theta_{fi}}-1)+i\pi\sum_{p_{f'}}\int H_{ff'}H_{f'i}(x+ye^{i\theta_{f'i}})\rho_{f'}d\Omega_{f'}\right]\rho_f d\Omega_f=0,\\&\delta y^*\sum_{p_i}\sum_{p_f}\int H_{if}e^{-i\theta_{fi}}\left[H_{fi}(x+ye^{i\theta_{fi}}-1)+i\pi\sum_{p_{f'}}\int H_{ff'}H_{f'i}(x+ye^{i\theta_{f'i}})\rho_{f'}d\Omega_{f'}\right]\rho_f d\Omega_f=0;\end{aligned} \tag{13}$$

whence we have

$$(a+ib)x+(a_1+ib_1)y=a,\quad (a_1^*+ib_1^*)x+(a+ib_2)y=a_1^*, \tag{14}$$

where a and b are given by (11) and

$$\begin{aligned}a_1&=\sum_{p_i}\sum_{p_f}\int H_{if}H_{fi}e^{i\theta_{fi}}\rho_f d\Omega_f=\rho_f\left[\frac{2\pi\hbar^2c^2}{EE_N(E_i^2-M^2c^4)}\right]^2\{\pi^2i[(AE_i+BMc^2)^2\\&\qquad+(BE_i+AMc^2)^2]+(4\pi/3)C^2(E_i^2-M^2c^4)\},\\b_1&=\pi\sum_{p_i}\sum_{p_f}\sum_{p_{f'}}\int\int H_{if}H_{ff'}H_{f'i}e^{i\theta_{fi}}\rho_f\rho_{f'}d\Omega_f d\Omega_{f'}\\&=4\pi^3\rho_f^2\left[\frac{2\pi\hbar^2c^2}{EE_N(E_i^2-M^2c^4)}\right]^3\frac{AE_i+BMc^2}{2}\{\pi_i[(AE_i+BMc^2)^2+3(BE_i+AMc^2)^2]\\&\qquad+(4/3)C^2(E_i^2-M^2c^4)\},\\b_2&=\pi\sum_{p_i}\sum_{p_f}\sum_{p_{f'}}\int\int H_{if}H_{ff'}H_{f'i}e^{i(\theta_{f'i}-\theta_{fi})}\rho_f\rho_{f'}d\Omega_f d\Omega_{f'}\\&=\pi^3\rho_f^2\left[\frac{2\pi\hbar^2c^2}{EE_N(E_i^2-M^2c^4)}\right]^3\frac{AE_i+BMc^2}{2}\{\pi^2[(AE_i+BMc^2)^2+3(BE_i+AMc^2)^2]\\&\qquad+(16/9)C^2(E_i^2-M^2c^4)\}.\end{aligned} \tag{15}$$

The differential cross section in this approximation, which we denote by $d\phi''$, is obtained by solving (15) and substituting the obtained values of x and y into the formula

$$d\phi''=d\phi_0|x+ye^{i\theta_{fi}}|^2. \tag{16}$$

Numerical results for the total cross section ϕ'' calculated from (16) have been given in the Table I. The agreement with the exact solution is better than in the first approximation. It has been

TABLE I.

p_0/mc	$g_1=g_2$ $\phi'(\text{cm}^2)$	$g_1=g_2$ $\phi''(\text{cm}^2)$	$g_1=g_2$ $\phi(\text{cm}^2)$	$g_1=g_2$ $\phi'(\text{cm}^2)$	$g_1=g_2$ $\phi''(\text{cm}^2)$	$g_1=g_2$ $\phi(\text{cm}^2)$
1	1.91×10^{-26}	1.91×10^{-26}	1.91×10^{-26}	2.25×10^{-26}	2.25×10^{-26}	2.25×10^{-26}
2	5.38	5.27	5.13	5.20	5.22	5.21
4	2.84	3.11	3.67	2.51	2.55	2.70
6	1.66	2.20	2.48	1.43	1.64	1.98
8	1.14	1.84	1.74	0.96	1.43	1.59

found, however, that our formulae (7) and (16) give angular distributions which do not agree very well with that given by the exact solution. For example, we have for $g_1=g_2$, $p_0/mc=8$,

$$\frac{d\phi'}{d\Omega_f}=0.0096(939+543\cos\theta_{fi})\times10^{-28}, \tag{17}$$

$$\frac{d\phi''}{d\Omega_f}=0.871(939+543\cos\theta_{fi})(0.0543+0.01146\cos\theta_{fi}-0.0493\sin\theta_{fi})\times10^{-28}, \tag{18}$$

which differ considerably from the exact formula

$$\frac{d\phi}{d\Omega_f}=(13.8+13.5\cos\theta_{fi})\times10^{-28}$$

in some directions. In order to get better agreement, it would be necessary to choose some more suitable function for U_{fi} or introduce more parameters.

PHYSICAL REVIEW VOLUME 67, NUMBERS 9 AND 10 MAY 1 AND 15, 1945

Proceedings of the Southeastern Section of the American Physical Society

MINUTES OF THE ATLANTA, GEORGIA, MEETING ON APRIL 6 AND 7, 1945

THE eleventh annual meeting of the Southeastern Section of the American Physical Society was held on a restricted basis in the Atlanta Biltmore Hotel and at the Georgia School of Technology, Atlanta, Georgia, on Friday and Saturday, April 6–7, 1945. Thirty-four out-of-town members and guests attended; local members and guests brought the attendance to approximately fifty persons. Local arrangements were made by a committee headed by E. E. Bortell.

The regular program consisted of ten papers, abstracts for three of which are appended hereto. Abstracts of the other papers will be found in a later issue of the *American Journal of Physics*.

Additional features of the program were: a Symposium on High Polymers (at which the following papers were presented: "The Chemical Characterization of High Polymers," by Kyle Ward, Jr.; "X-Ray Diffraction as Applied to the Study of Semi-Crystalline Materials," R. C. L. Mooney; and "The Relation of Physical Properties to the Molecular Character of High Polymers," Emil Ott); a review of the American Association of Physics Teachers meeting recently held in New York, by D. R. McMillan;

and an informal panel discussion, following the annual dinner, on the general topic of the training of physicists for work in industry.

At the business meeting the election of the following officers for the Section was announced: Chairman, F. L. Brown; Vice-Chairman, R. C. L. Mooney; Secretary, E. Scott Barr; Treasurer, C. B. Crawley; and Member of the Executive Committee, A. E. Ruark.

The time and place for the 1946 meeting are to be announced later.

E. SCOTT BARR, *Secretary*

ABSTRACTS OF CONTRIBUTED PAPERS

1. A Modification of Kavanau's Relation. R. T. LAGEMANN, *Emory University, Emory University, Georgia.*—A recent equation by Kavanau[1] relates interatomic distance and bond multiplicity for a pair of atoms, whether these atoms occur in diatomic or polyatomic molecules. Examination of the constants of that equation shows them to be related to the sum, M, of the atomic weights of the atoms making up the bonded atom pair. If the constant b is set proportional to M and the constant a inversely proportional to M, we have

$$D=\frac{K_1}{M}+K_2M\left(\frac{n_1+n_2-1}{n_1+n_2+1}\right)^N$$

where D is the interatomic distance, N the bond multiplicity, and n_1 and n_2 the principal quantum numbers of the valence electrons. K_1 and K_2 are constant for all pairs of atoms having the same value of n_1 and the same value of n_2. For pairs of atoms where $n_1=n_2=2$ the calculated values of the interatomic distance are given by this new relation with an average deviation of 0.03 angstroms from the observed values.

[1] J. L. Kavanau, J. Chem. Phys. 12, 467 (1944).

2. Air Resistance Bridge for Measuring Fiber Properties. K. L. HERTEL, *University of Tennessee, Agricultural Experiment Station.*—The ratio of the external surface of a fiber to its volume may be used as a measure of fiber fineness. The resistance offered to air flow by fibers confined in a tube with perforated ends is a function of the tube cross-section, length of fiber wad, air viscosity, fiber orientation, fiber surface per unit volume, and porosity of the fiber wad. A predetermined mass of fibers in a cylindrical tube with perforated ends constitutes one resistance, and three capillary tubes the other resistances of an air "Wheatstone bridge." Air pressure of about two centimeters of water produced by an aspirator bulb and slack bellows provides the potential difference, while an inclined kerosene-filled manometer takes the place of the galvanometer and indicates the balance of the bridge. The fiber wad is compressed first to balance a low standard resistance and then a high standard resistance. The corresponding wad-lengths, along with constants of the instrument, furnish the necessary data to determine the fiber surface per unit volume or per unit mass and the density of the fiber material.

3. Grid Control of X-Ray Tubes. R. PEPINSKY, *Alabama Polytechnic Institute* (on leave at the Radiation Laboratory, Massachusetts Institute of Technology).—Addition of control grids in x-ray tubes provides advantages which have been utilized by Bouwers[1] and others in deep-therapy and radiographic work, and recently by Eisenstein[2] in diffraction investigations. Some properties of grid-controlled operation are considered, and two further applications to diffraction studies are discussed. In the first of these, the grid is biased below cut-off and pulsed to produce bursts of electron current and x-radiation of high peak intensity. The pulses are phased to any desired portion of some cyclic lattice distortion, such as that produced by the mechanical flexing of a material or the oscillations of a piezoelectric crystal, and atomic displacements are observed throughout the cycle. To permit observations at any frequency and phase, the high voltage is rectified and filtered; a storage condenser is provided of capacity proportionate to pulse-duration.

In the second application, grid-control serves to stabilize x-ray output. One beam from a multi-port tube (operated either on direct or pulsating current) is monochromatized and received by a Geiger counter or ionization chamber. The amplifier output is then fed back to the grid in such a manner as to maintain a monochromatized beam of fixed intensity.

[1] A. Bouwers, Arch. d'Elec. Med. 39, 376 (1931).
[2] A. Eisenstein, Rev. Sci. Inst. 13, 208 (1942).